ANALYSIS OF WIND EFFECTS ON TALL BUILDINGS OF IRREGULAR CROSS-SECTIONS USING NUMERICAL SIMULATION

A DISSERTATION
SUBMITTED IN PARTIAL FULFILMENT OF THE REQUIREMENTS FOR THE AWARD OF THE DEGREE OF

MASTER OF TECHNOLOGY
IN
STRUCTURAL ENGINEERING

Submitted by:

Arya S M

2K21/STE/08

Under the supervision of

RITU RAJ

DEPARTMENT OF CIVIL ENGINEERING

DELHI TECHNOLOGICAL UNIVERSITY

(Formerly Delhi College of Engineering)

Bawana Road, Delhi- 110042

MAY, 2023

DEPARTMENT OF CIVIL ENGINEERING
DELHI TECHNOLOGICAL UNIVERISTY
(Formerly Delhi College of Engineering)
Bawana Road, Delhi – 110042

CANDIDATE'S DECLARATION

I, ARYA S M, 2K21/STE/08, student of M. Tech (Structural Engineering), hereby declare that the project Dissertation titled "**Analysis of wind effects on tall buildings of irregular cross-sections using Numerical Simulation**" which is submitted by me to the Department of Civil Engineering, Delhi Technological University, Delhi in partial fulfilment of the requirement for the award of the degree of Master of Technology, is original and not copied from any source without proper citation. This work has not previously formed the basis for award of any Degree, Diploma Associateship, Fellowship or other similar title or recognition.

Place- Delhi
Date:

ARYA S M

DELHI TECHNOLOGICAL UNIVERISTY
(Formerly Delhi College of Engineering)
Bawana Road, Delhi – 110042

CERTIFICATE

I hereby certify that the Project Dissertation titled "Analysis of wind effects on tall buildings of irregular cross-sections using Numerical Simulation" which is submitted by ARYA S M, 2K21/STE/08, Department of Civil Engineering, Delhi Technological University, Delhi in partial fulfilment of the requirement for the award of the degree of Master of Technology, is a record of the project work carried out by the student under my supervision. To the best of my knowledge, this work has not been submitted in part or full for any Degree or Diploma to this University or elsewhere.

Place: Delhi
Date:

Dr. RITU RAJ
SUPERVISOR
Assistant professor
Department of Civil Engineering
Delhi Technological University
Bawana road, Delhi - 110042

ABSTRACT

Unavailability of land is an important issue that is to be given due concern, as there is high possibility for this issue to reach an uncontrollable extent due to the increasing population. Authorities are taking possible actions to bring a reduction to these problems, of which construction of high-rise structures is one of the most accepted one. Trends have changed from normal conventional regular structures to irregular shaped high-rise buildings due to land concerns as well as its aesthetic features. But rapid and faster constructions lack proper checking of the structures for dynamic loadings such as wind loads. Unavailability of enough data for irregular structures in codal provisions is also a major limitation, which calls for other effective methods like wind tunnel testing or numerical simulations. Among these alternatives numerical simulations are widely adopted due to its quick and effective nature.

This paper deals with wind analysis on two different 'fish'-shaped models for isolated conditions as well as under interference effect. CFD simulation is done in Ansys CFX for different wind incidence angle ranging from 0°-180°. The interval is taken as 15°. The model is of cross-sectional area 400m^2 with a height of 60m and is modelled at a scale of 1:100. The variation of Cp at every face of the model at different wind incidence angle, pressure contours for both the models under isolated conditions, horizontal streamlines, comparison of Cp of model under isolated and grouped condition and drag force coefficients of model under isolated conditions are found at the result part. It is found that the face on the windward side experiences more positive pressure when the wind is directly perpendicular to the face of the building. It is also concluded that the interference effect improves the performance of the building.

ACKNOWLEDGEMENT

I would like to express my sincere gratitude to my supervisor **Dr. Ritu Raj** (Assistant professor, Delhi Technological University) for the continuous support for my MTech study and research, for his patience, motivation and guidance.

I extend my heartiest gratitude to **Mr. Deepak Sharma** (PhD Scholar, Delhi Technological University) for his constant support and help throughout my work. I am sincerely thankful to all the teachers who have ever taught me, who gave me strength, courage and knowledge to reach where I am.

I have no words to express my appreciation for the unbound love and support from my family and friends, who have helped me to overcome any obstacles during the course of my work.

ARYA S M

TABLE OF CONTENTS

LIST OF TABLES

LIST OF FIGURES

LIST OF PHOTOGRAPHS

ABBREVIATIONS AND SYMBOLS

ABBREVIATION	DESCRIPTION
CFD	Computational Fluid Dynamics
SST	Shear Stress Transport
IS	Indian Standards
C_p	Coefficient of pressure
C_d	Drag force coefficient

CHAPTER 1

INTRODUCTION

1.1 GENERAL

Tall buildings or towering structures are an important requirement in this modern era due to rapid uncontrolled increase in population and lack of available usable land area. Authorities are finding it difficult to find regular shaped plots for the construction of buildings, which resulted in a change from conventional symmetrical structures to the construction of more and more irregular structures. Tall structures are very much prone to dynamic loadings such as earthquake loads, wind loads, etc. So having an idea on the nature of effects of these loads on the structure is very important during its design as well as service stages. But it is always a challenge for engineers to find the wind effects due to unavailability of wind data. On top of that, finding the distribution of wind loads on irregular plan shaped structures are also a difficult task, since shapes of structures also have effect on resistance to wind loads. The wind loads are such that, it increases with height. Tall buildings in the modern era are very vulnerable to dynamic wind loads, which have a negative impact on serviceability. These massive formations are man-made bluff bodies. Wind-induced excitations caused by the bluffness of the building geometries cannot be ignored in the case of a bluff bodies. Tall buildings which are slender in nature shows very high flexibility which causes them to vibrate under the action of wind loads and results in movement of buildings.

The shortage of available land for buildings also resulted in construction of structures in group. Circulation patterns around two or more tall structures are more complex than flow patterns surrounding solitary buildings due to interaction effect. Neighbouring structures can reduce or enhance flow-induced forces on a building, depending on its shape and arrangement, orientation with respect to the direction of flow, and upstream terrain conditions. Therefore, it's very important to look into this effect of interference during

the design phase. Consideration of interference effect will be an important factor in future due to increasing dense arrangement of all the structures.

Burj Khalifa

John Hancock Centre

Taipei 101

Turning Torso

Evolution Tower

Al-Hamra Tower

Willis Tower

Photo 1.1. Different tall buildings in the world

The effect of wind load on tall buildings can be either found out through a wind tunnel experiment or with the help of numerical study using computational fluid dynamics. The use of wind tunnel is reducing due to its unavailability and expenses. On top of that, the experimental study using wind tunnel is time consuming. So, most of the recent studies on wind analysis is done on computational fluid dynamics software due to its reliable fast and accurate simulations. As the wind tunnel experiments call for the installation of sophisticated sensors and it is just limited to few points inside the installed setup, the effect of vortex shedding and turbulence wake are not taken into account.

A large variety of variables are involved in building modelling, including height, plan cross sectional shape, building shape, distance between surrounding structures, wind incidence angles, topographical features, and numerous metrological circumstances.

1.2 WIND LOAD

Wind is the movement of air in the atmosphere and it mainly occurs due to the difference in pressure between two different spots. The wind may be of two types namely: Rotating and non-rotating. The rotating wind occurs due to tropical cyclones whereas the non- rotating occurs due to normal pressure difference in wind direction. Wind load is the load exerted by wind on any structure in its flow direction and it is predominantly a horizontal force. The wind provides overpressure on the windward side, while it creates suction on the leeward side. It acts along the height of the building and is a primary load on tall structures. The action of wind load on a structure is mainly determined by two important parameters: Structural and flow parameters. The flow parameters mainly include the velocity of flow, flow direction, ground characteristics etc. Height of the structure, its aspect ratio, presence and orientation of nearby structures, openings in buildings, etc, are considered under structural parameters. The distribution of wind load is not uniform throughout the building elevation and is affected by ground friction. The surface friction decelerates the wind flow at ground level. It varies from zero at the surface and grows with elevation until it reaches a point known as the gradient height, where friction from the earth's surface has no effect on it and it achieves its "gradient velocity".

1.3 WIND LOAD CALCULATION

The numerical and experimental methods of calculation of wind load have been already discussed. The theoretical calculations are always done on the basis of Indian Standard

codes and the code which comes under this is IS: 875 (part- 3)- 2015. The drawback associated with the standard code is that it provides the wind load calculation for conventional symmetrical shapes and not for the irregular shapes which are mostly used today. Pressure coefficient method and force coefficient method are mainly adopted in codal provisions.

The design wind force or load which acts on a structure is found from the equation,

$$F = A * P \tag{1.1}$$

where,

F – design wind load

A – area

P – total wind pressure acting on the area A and is given as,

$$P = C_p * P_d \tag{1.2}$$

where,

C_p - coefficient of pressure from code

P_d - design wind pressure, the formula for which is given as,

$$P_d = K_d K_a K_c P_z \tag{1.3}$$

where,

K_d – directionality factor for wind

K_a – area averaging factor

K_c – combination factor

P_z – design wind pressure at a known height z (N/m^2) and is given as,

$$P_z = 0.6 * V_z^{\,2} \tag{1.4}$$

V_z – design wind velocity at height z (m/s) and is given by,

$$V_Z = V_b k_1 k_2 k_3 k_4 \tag{1.5}$$

where,

V_b – basic wind speed

k_1 – probability factor

k_2 – terrain roughness and height factor

k_3 – topography factor

k_4 – cyclonic regions importance factor

When it comes to the case of a building with openings the coefficient of pressure is taken as the difference between external and internal pressure coefficients. The formula is given below:

$$C_p = C_{pe} - C_{pi} \tag{1.6}$$

where,

C_{pe} – external coefficient

C_{pi} – internal coefficient

And hence the wind pressure is given as,

$$P = (C_{pe} - C_{pi})P_d \tag{1.7}$$

When force coefficient is considered instead of pressure coefficient, the wind load or force is given as,

$$F = C_f A_e P_d \tag{1.8}$$

where,

C_f – force coefficient

A_e – effective frontal area of the building considered

1.4 EXPERIMENTAL METHOD

As we have already discussed the standard codes will only help in the load calculation for symmetrical shaped structures, which always leaves a question in the case of unsymmetrical irregular structures. Also, the reliability of the calculated loads from the codes are to be cross checked with results from other methods. The geometry of normal structures, topographical characteristics, and other adjacent structures complicate wind flow, necessitating experimental evaluation of wind forces employing wind tunnel studies on the scaled model and simulated wind. The experimental study done on a wind tunnel also ensures proper safety to resist aerodynamic instabilities in case of tall buildings under study. It also gives more accurate results on torsional velocities which ensures good comfort during the service life of the structures.

1.5 NUMERICAL SIMULATION

Computational fluid dynamics can be easily used for the analysis of all types of buildings including, regular and irregular shaped buildings. The validation of result from numerical

simulation is to be done with standard codes or experimental results, so as to confirm that the values assigned for the building simulation is appropriate and matches with the natural wind conditions. In CFD, the building under study is divided into number of elements with the help of meshing. The number of elements can be controlled by changing the mesh size. Meshing also determines the shape of elements. The solution is obtained when the simulation runs and the results depends on the flow parameters which were set before running the analysis. The results are obtained from the post CFD tab where the data is available to be exported to excel sheet, from where various parameters can be obtained using equations.

1.6 NEED OF THE STUDY

Wind action on a building is unpredictable and it is always varying. The wind forces are such that it increases with height and causes a critical condition in case of high-rise structures. So, it is very important to study and understand the behaviour of these structures under wind actions using standard codes, wind tunnel experiments or numerical analysis. This study makes use of numerical simulation as it is less expensive, time saving and gives accurate results. The use of standard codes limits the study to just conventional regular plan-shaped buildings, which makes it an ineffective method to adopt.

Few gaps were observed during literature study. Studies were done on irregular shaped buildings, but only few studies were done on interference study on tall irregular buildings of equal area and height. Comparative study of pressure distribution on a model in both isolated state and under interference condition is rarely done. Variation in force coefficients between two different models having a small change in corner cuts haven't been done.

In this project, two different Fish shaped buildings are taken and the wind analysis on the structures have been done. The experimental works for the selected shapes have been done already, which calls for the numerical analysis for the same to be done to check the reliability of the data obtained from wind tunnel analysis. This also ensures that the real wind parameters can be incorporated into virtual wind tunnels.

1.7 OBJECTIVES

Several research gaps were observed during the literature study and the following objectives were drawn out from it:

1. To incorporate actual wind parameters like wind velocity, flow intensity etc, into a virtual wind tunnel, which aids in numerical analysis.
2. To validate the data and procedures used in the study using IS code.
3. To study the effect of interference on the building performance in terms of pressure coefficient and comparing it with isolated conditions. Four different interference conditions are used in the present study.
4. To plot the variation in pressure coefficient on a single face at different wind incidence angle.

1.8 DIVISION OF THESIS

CHAPTER-1 explains the effect on tall building and a briefing on wind load calculations. The need of present study and the objectives taken is also given in this chapter.

CHAPTER-2 reviews various papers which were taken to carry out the study. The information from these papers formed the basis for the project.

CHAPTER-3 gives the step-by-step procedure followed in this study. The shape taken, adopted model etc are also discussed.

CHAPTER-4 discusses the obtained results from simulation and graphs are plotted. Contours and velocity streamlines are also shown.

CHAPTER-5 draws the conclusions from the obtained results. The future scopes of the study are also discussed.

CHAPTER 2

LITERATURE REVIEW

2.1 GENERAL

The objectives of the present study have been taken from the gap observed in papers which are already available. Since this project is on force and pressure analysis on tall structures, papers related to study on same have been selected. Also, papers discussing interference effects on tall buildings as well as CFD simulation are also taken. The wind action is considered such that the wind acts on building at various wind incidence angles. The standards and codes which are used for the validation purpose are also included.

2.2 PROVISIONS FROM CODE

The codes and standards are taken for the validation purpose of square or rectangular models. IS 875:part-3:2015 [1] is used to crosscheck the pressure coefficient value obtained for the selected square model, so as to confirm the reliability of the CFD parameters. The IS codes limits the results on the pressure coefficient values of regular shaped buildings and irregular shaped buildings are not considered. The wind incidence angle is taken from 0° to 90°.

2.3 RESEARCH STUDIES

Sheng et al. [2] did an experimental study to investigate the unstable properties of global and local wind loads, as well as their connections with the approaching atmospheric boundary layer, using wind tunnel measurements on a high-rise building with a clearly established atmospheric boundary layer at a scale of 1:300. It was observed that inlet circumstances influence the velocity and level of turbulence. The front face is constantly affected by upstream flow, whereas the lateral faces are affected by vortex shedding. The behaviour varies depending on the ground conditions.

Bhattacharjee S et al. [3] examined the advantages and disadvantages of employing irregular type butterfly plan-shaped buildings over standard square plan-shaped structures are examined in this study. The numerical model was validated using two turbulence models, standard k-epsilon (SKE) and shear stress transport (SST). Contours and horizontal lines were taken to analyse the pressure fluctuation along building facades. The overall plan area used by the building increases as the irregularity ratio increases, despite the fact that the ventilation of the building improves dramatically, as does the force coefficient operating on the building and the maximum local suction at the corner regions.

Merrick et al. [4] investigated the effect of building shape on the wind-induced reaction of a structure through detailed wind tunnel analysis. Square, rectangular, elliptical, triangular and circular shapes were taken. Torsional effect on these shapes were analysed and it was found that rectangular, elliptical and triangular are more prone to loading due to torsion.

Li et al. [5] experimented on a L-shaped model using a wind tunnel to find the effect of terrain condition on mean torque coefficient. It was found that the terrain categories have no influence over it and also the RMS torque coefficient was found to be proportional to wind velocity. The mean and RMS base torsional moment coefficients, which fluctuate with approaching wind direction, follow the same patterns as the torque coefficient.

Ming et al. [6] carried out wind tunnel experiments to study wind resistant aspects of high-rise buildings. The pressure and forces were analysed. The effect of wind under interference condition was also studied. The wind resistance of building was explained using examples.

Bhattacharyya et al. [7] did an experimental study on a E- shaped tall buildings with 3 interconnected wings. The study was done to find the wind induced pressure on the structure and it was observed that the induced pressure depended on various factors such as the geometry of the building, the wind incidence angle, intensity of the turbulence caused by the wind etc. It is also concluded that future scope for enhancement of the resilience properties of E-shaped buildings were also be considered.

Yi J et al. [8] did a wind tunnel study as well as full scale studies on a super-tall building to study the wind effects. The paper discussed the effect of pressure and pressure distribution, load assessment, dynamic response and vibration mitigation. The data obtained from the study was also used to refine the design approaches. The findings also contributed to development of design guidelines, which ensures proper comfort of the occupants.

Chakraborty et al. [9] experimented on a '+'- plan shaped building model in a wind tunnel setup. The study scale was taken as 1:300 and the wind incidence angle were taken between 0°-45°. The pressure coefficient on every face were determined and large variation in pressure distribution is obtained on faces affected by eddies formed due to flow separation. CFD analysis were also done using ANSYS and a comparison was done between both the methods. It was observed that the numerical simulation results were in good agreement with the experimental results.

Paul et al. [10] studied the behaviour of various faces of a Z-shaped building under the action of wind acting at different angles. Numerical simulation was done to determine the force coefficients as well as pressure coefficients. The angles were taken at an interval of 30° for a range of 0°-150°. The paper also presented the wind flow pattern showing area of vortex formation and the corners at which the separation of flow occurs. Contours are also incorporated to show the pressure distribution.

Raj et al. [11] did experimental study on buildings having different cross-sectional shapes but having equal area. The study was done on base shear, base moment and twisting moment and it was concluded that these results were influenced not just by wind angles, but also by the geometry of the structure.

Jb et al. [12] presented a wind tunnel study to determine the effect of an adjacent structure on the pressure distribution of a tall structure. Local values of the external pressure coefficient on the leeward wall, near to the gap between buildings, have been shown to be 2.5 times higher for specific wind directions than on an isolated building. This may also cause a reverse circulation in the apartment buildings natural ventilation system.

Oliveira et al. [13] demonstrated that the consideration of a 2-D flow field at the middle of the building span results in a greater suction at the roof of building as well as on its leeward face. Guidelines are also given for mesh distribution and effective sizing of domains on which the building dimension is related to.

Patel et al. [14] analysed the pressure distribution along a differential height structure. To determine the optimum length to be selected for a building, a comparative study was done on buildings with varying lengths. The optimum length is selected by analysing the pressure distribution at mid length.

Mukherjee et al. [15] did both wind tunnel experiment and numerical simulation to analyse the wind effect on same model. In CFD study, both the models namely: k-ε model and shear stress transport model (SST) were selected. The SST model showed a good agreement between experimental and numerical results. Also, the results obtained from SST model was found to be of higher magnitude. Change in pressure distribution was also observed in case of interference effect.

Verma et al. [16] did an experimental study to analyse the effect of wind at different angles on a square shaped tall structure. An increase in pressure was seen along the height of building in case of positive pressure, whereas an increase from windward side to leeward side was observed for negative pressure. Pressure contours were used to show pressure distribution and the data obtained were used for design of structural frame and wall claddings by designers.

Kumar Bandi et al. [17] did wind tunnel experiment on 26 different models of varying shapes. The different shapes were triangular, square, pentagon, hexagon, etc. the effect of various shapes on the peak pressure acting on structures were analysed. Few twisted models were also taken and twist angle was considered. It was observed that shape and twist angles showed great difference in peak pressure.

Nagar et al. [18] experimented on a H- shaped tall building in a wind tunnel to find out the mean pressure coefficients. Interference effect is also analysed by the installation of a

square model adjacent to the H-shaped building. It was observed that more pressure was obtained on the H-shaped building. It was also observed that full blockage interference condition generated more suction.

Kar et al. [19] studied the variation in pressure distribution on every face of an octagonal plan shaped building due to the interference effect caused by three different square shaped buildings of equal height. The channelling and shielding effect due to adjacent building on the octagonal buildings are also noted. The behaviour of faces becomes more systematic as the distance between the octagonal building and farthest square shaped building is increased.

Pal et al. [20] did an experimental study on Fish shaped tall buildings under isolated condition. The pressure coefficients are obtained for a wind incidence angle ranging between 0°-180°. It was observed that higher magnitude of suction and pressure coefficients were observed in case of 30°, 60°, 120° and 150°. It is also concluded that the orientation at 90° is to be avoided due to higher overturning moment coefficients.

Meena et al. [21] determined the effect of corner configurations on the overall performance of buildings against wind action. Different configurations like corner cut, rounded corner etc were selected and numerical simulation was done. The configurations showed a good effect in case of drag and lift forces, where it was reduced to an acceptable level. It was also observed that pressure distribution along windward direction does not depend on the height of the structure.

Kumar et al. [22] analysed the wind pressure distribution on an irregular octagonal plan shaped building model using numerical simulation. The geometry was added with a central opening to increase the surface area for higher ventilation. Different characteristics of wind flow such as separation of flow, re-attachment, vortex formation and wake regions were considered. Different wind incidence angles were taken and it was observed that at every angle suction was created at the central opening.

Goyal et al. [23] demonstrated a detailed study on various results obtained from the numerical simulation of a Y-shaped building model. Velocity streamlines, pressure coefficients, pressure distribution and turbulent kinetic energy at various wind angle were studied. The Y- shaped model was also modified by giving rounded corners, so as to do a comparative study. It was concluded that higher wind load resistance was observed in case of Y-shaped building with rounded corners.

Ming Lam et al. [24] applied CFD to study the wind action as it flows along rows of three similar square shaped tall buildings. It was concluded that interference effect is mainly observed due to channelling of wind flow path by the gaps between the building, as a result of which suction is observed on faces near to gaps.

Sobankumar et al. [25] focused on CFD analysis of pentagonal shaped tall buildings to determine the external pressure coefficients and drag and lift coefficients. It was observed that the maximum pressure coefficient was observed on Face A at 180° wind incidence angle and minimum on Face D at 135°.

Bairagi et al. [26] did numerical simulation to understand the wind effect on a stepped tall building. Four different model of same height, but of different set back distance was taken and analysed. It was observed that in all the cases, the maximum pressure was observed at a height of 90% of total model height. Also, the steps in the model also varies the turbulent intensity of wind flow. The negative pressure was mainly seen on the roof of the buildings. The study concluded that the data obtained can be used for the design of roofs of such similar buildings.

Raj et al. [27] studied the performance of plus- shaped and square shaped building models under the action of wind loads. It was observed that, when the wind hits perpendicular to the windward face, the windward face experience a positive pressure, on the other hand al the other face experience suction. The pressure observed is maximum on top part of building face, since the wind velocity is greater at that height. Most surfaces have suction at skew angles and when wind blows perpendicular to a short wall.

Meena et al. [28] did numerical simulation of hexagonal and octagonal shaped buildings to determine the effect of shape on wind effects. Pressure coefficients, streamlines and contours were obtained 0°. Similar variation in pressure distribution is observed in case of both the models for windward faces.

Thordal et al. [29] outlines the critical factors to consider when using CFD models to determine wind loads on high-rise buildings. A significant difference between CFD and wind tunnel results is mostly determined by inflow conditions. CFD findings can be compared to wind tunnel data if the exact identical boundary conditions are employed in the simulation; otherwise, severe errors and misleading results can occur. The fluctuating pressure coefficient is more likely to be influenced by the velocity and turbulent intensity profiles, whereas the fluctuating pressure is mostly influenced by the turbulence intensity. Isolated buildings which are often thin and have a reduced width to depth ratio, the flow will separate at the leading edge and will not reconnect to the side surfaces.

Revuz et al [30] challenged the domain size guidance which are in use by providing a different domain size around the building. The reliability of the new dimension was checked on the basis of velocity field and pressure coefficients obtained. It was observed that a domain of size which is almost 10% of the size of domain followed in existing guidelines can be used at just a loss of less than 10% accuracy.

2.4 LIMITATIONS

It is observed from the literature review that number of studies have been done on regular as well as irregular plan shaped buildings using wind tunnel experiments or numerical simulations. But only few studies were done on the interference part and taking two buildings of same shapes keeping one as main building and the other as instrumental building is rarely done.

This study deals with the numerical simulation of two different fish shaped building models (S1 and S2) both in isolated condition and under interference effect. The wind incidence angle is taken from 0°-180° at an interval of 15°. Four different interference conditions are adopted here and are as follows: Front to Front (F-F), Back to Back (B-B), Back to front (B-F) and Front to Back(F-B).

CHAPTER 3

METHODOLOGY

3.1 GENERAL

This study mainly aims on the CFD analysis of two different fish-shaped buildings using ANSYS under isolated as well as interference effect. This chapter includes the step-by-step process involved in the completion of the simulation part.

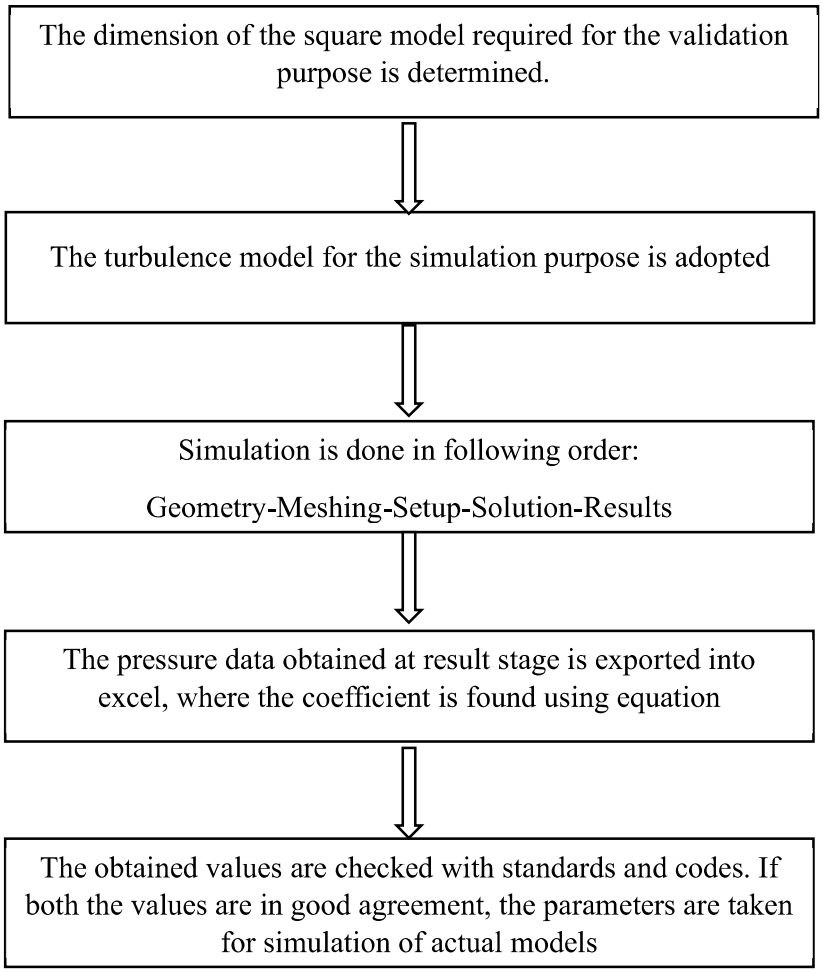

Fig 3.1. Flowchart depicting workflow

3.2 NUMERICAL ANALYSIS

As discussed earlier, the study of wind effects on tall buildings can be either done on a boundary layer wind tunnel or with the use of numerical simulation software. The use of numerical method is mostly preferred nowadays because of the easiness with which it can be done and the economic part of it. The various parameters which are used in the analysis is taken after validating it with the existing standard codes and the results obtained from the simulation is to be crosschecked with experimental data to check the reliability of the given conditions. The turbulence model considered in this study is the k-ε turbulence model.

The wind flow is generally considered as an unsteady flow where the pressure, velocity etc, varies in all three coordinate directions. In general, the 3-D unsteady flow in case of fluid is generally governed by Navier-Stokes equation. It consists of mainly two equations namely: continuity equation and momentum equation. These two equations help in determining the characteristics of flow and turbulence effect in fluid flow.

The turbulence model that are available is of two types: zero-equation model and two-equation model. The zero-equation model is simpler and quickly solved, but it uses constant eddy viscosity throughout the calculation unless a change is made. In case of two-equation models, two different equations have to be solved to generate solution.

Coming to the turbulence model in order to match the real natural scenarios, k-ε model is selected for this study as it is identified as the most appropriate among all. The k-ε model is a two-equation model and it connects the Reynolds stresses to mean velocity gradients as well as with turbulent viscosity. Here, the k represents the turbulent kinetic energy and ε is the turbulence eddy dissipation. It has the advantage of not incorporating any geometry-related characteristics into the modelling.

The turbulent kinetic energy is given as,

$$k = \frac{1}{2}\left(\overline{u'^2} + \overline{v'^2} + \overline{w'^2}\right) \tag{3.1}$$

and the turbulence eddy dissipation is given as,

$$\varepsilon = \frac{k^{3/2}}{0.3D} \tag{3.2}$$

Navier-Stocks equation is,

$$\frac{\partial(\rho u_i)}{\partial t} = -\frac{\partial(\rho u_i u_j)}{\partial x_j} - \frac{\partial P}{\partial x_j} + \frac{\partial}{\partial_{x_j}}\left[\mu\left(\frac{\partial_{u_j}}{\partial_{x_j}} + \frac{\partial_{u_j}}{\partial_{x_j}}\right)\right] + F \tag{3.3}$$

The continuity equation:

$$\frac{\partial_\rho}{\partial_t} + \frac{\partial_{\rho_i}}{\partial_{x_i}} = 0 \tag{3.4}$$

and the momentum equation is given as,

$$\frac{\partial(\rho U_i)}{\partial t} = -\frac{\partial(\rho U_i U_j)}{\partial x_j} - \frac{\partial p'}{\partial x_i} + \frac{\partial}{\partial x_j}\left[\mu_{eff}\left(\frac{\partial_{U_i}}{\partial_{x_j}} + \frac{\partial_{U_j}}{\partial_{x_i}}\right)\right] + S_M \tag{3.5}$$

where,

S_M – total sum of body forces

μ_{eff} – effective viscosity related to turbulence

p' - modified pressure and is given as,

$$p' = p + \frac{2}{3}pk + \frac{2}{3}\mu_{eff}\frac{\partial U_k}{\partial x_k} \tag{3.6}$$

$$\mu_{eff} = \mu + \mu_t \tag{3.7}$$

μ_t – turbulent viscosity and is given as,

$$\mu_t = C_\mu \rho \frac{k^2}{\varepsilon} \tag{3.8}$$

C_μ is the k-ε model constant and the value is taken as 0.09

On the basis of continuity and momentum equations, k and ε are given by the equation below:

For turbulent kinetic energy,

$$\rho\frac{\partial(u_i k)}{\partial x_i} = P_k + P_b - \rho\varepsilon + \frac{\partial}{\partial x_i}\left[\left(\mu + \frac{\mu_t}{\sigma_k}\right)\frac{\partial k}{\partial x_i}\right] \tag{3.9}$$

For turbulent dissipation,

$$\rho\frac{\partial(u_i\varepsilon)}{\partial x_i} = \frac{\partial}{\partial x}\left[\left(\mu + \frac{\mu_t}{\sigma_\varepsilon}\right)\frac{\partial\varepsilon}{\partial x_i}\right] + C_1\frac{\varepsilon}{k}(P_k + C_3P_b) - C_2\rho\frac{\varepsilon^2}{k} \tag{3.10}$$

Here, C_1, C_2, C_3, σ_ε and σ_k are k-ε turbulent model constants.

P_k – buoyancy production term

For flow which are incompressible,

$$P_k = \mu\left(\frac{\partial U_i}{\partial x_j} + \frac{\partial U_j}{\partial x_i}\right)\frac{\partial U_i}{\partial x_j} \tag{3.11}$$

Cases where the flow changes continuously, this model cannot be used. And it cannot be used in case of rotating flows.

The other turbulence models which are used in practice other than k-ε model are: k-ω model and shear stress transport (SST) model. The SST turbulence model is mostly used in case of low-rise buildings.

3.2.1 MEAN VELOCITY CONSIDERATION

Wind does not flow consistently in nature. Wind speed increases as height from the earth increases due to less friction exerted by roughness created by plants and structures on the ground in the ABL profile. As a result, the wind flow encountered in high-rise buildings is not consistent over the building's height. The different equations which govern wind flow are given below:

1. Parabolic law:

$$u = u_{Ref}\sqrt{\frac{Z+22}{Z_{Ref}+22}} \tag{3.12}$$

where,

u_{Ref} – reference wind speed (m/s)

Z_{Ref} – reference height (10m)

u – wind velocity at a height 'z' m over ground surface

2. Power law:

$$u = u_{Ref}\left(\frac{Z}{Z_{Ref}}\right)^{\propto} \tag{3.13}$$

α – terrain roughness coefficient

Power law is a modification of parabolic law, but it has some limitations. Since its simple and easy to use, it is more commonly used.

3. Logarithmic law:

$$u = \frac{1}{k}u_0 L_n\left(\frac{Z-Z_d}{Z_0}\right) \tag{3.14}$$

k - Von Karman constant (0.4)

u_0 – friction velocity $\left(u_0 = \sqrt{\frac{\tau_w}{\rho}}\right)$ (3.15)

where,

τ_w – wall shear stress

ρ – density of air

Z_0 - roughness length

Z_d – zero plane displacement

This law is used in case of buildings with height less than 10m.

3.2.2 GEOMETRY

The models taken in this study is different from the conventional symmetric models that is commonly used. Two fish- shaped models having same cross-sectional area and height is taken. The models are to be analysed both in isolated as well as under interference effect. The shapes taken for the study is shown below:

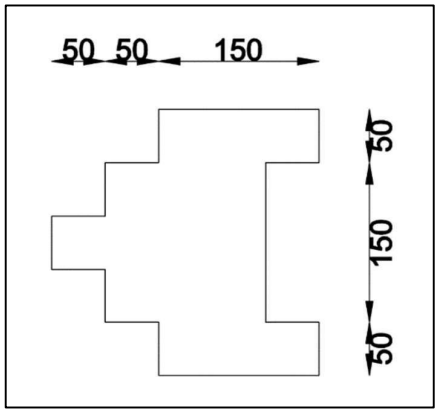

Model 1 (S1)

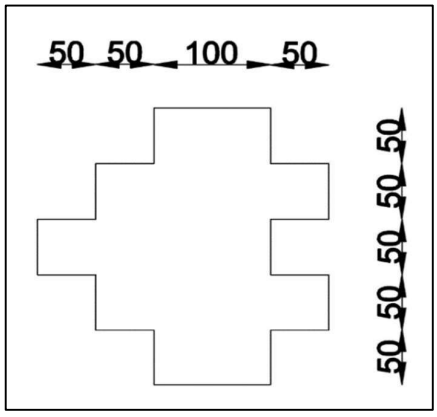

Model 2 (S2)

Fig 3.2. Shapes taken for the study

In the geometry stage, the structure is modelled in a scale of 1:100. The cross-sectional area of the model taken is 400m^2 and the height is 60m. In the design modeller, the structure is designed with the same area of 40,000mm^2 and a height of 600mm. Once the

modelling is done, the domain has to be established around the building model. The domain here is the virtual wind tunnel which forms the path for the wind flow.

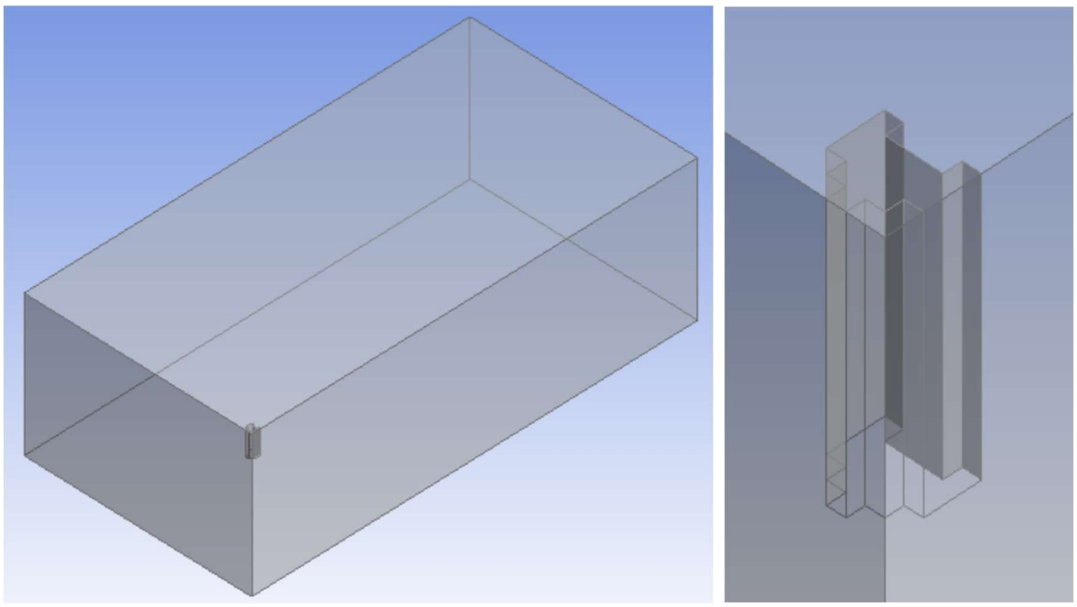

Fig 3.3. Model inside domain

The domain size is chosen so that the model placed within it has no effect on its boundaries, that is, the computational domain is kept big enough to avoid reflection of fluid streams. The domain size here is taken according to the domain size recommendation in Revuz et al. [30]. Consideration should be given to optimise the domain size. It should not be too large, since this will necessitate a greater number of computational cells for analysis, which will take more time and demand more processing power for the solution to converge. The dimension of the domain should be given such that, the size in flow directions as well as the side wall of domain should be 5H distance from the face of the building, where H is the height of the building. The distance behind the model is kept at 15H, so as to form the space for the vortex and wake generation. The height of the domain above surface is taken as 6H. The dimensions of the domain are given below.

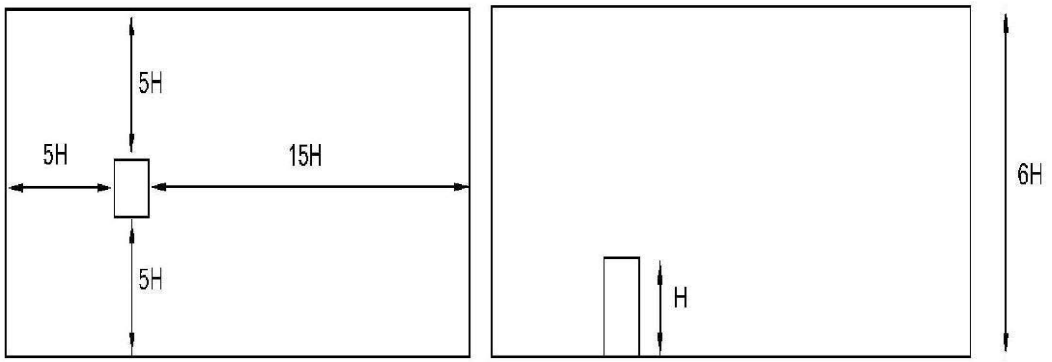

Fig 3.4 Domain Size

The wind effect on building under interference effect is also being taken into consideration in this study. The presence of an adjacent structure influences the various wind effects on a building. The gap between the buildings will act as a pathway for the wind flow. Here, both the models are studied under interference effect. The main building is placed along with an instrumental building and the four different interference conditions are taken namely: Front to Front, Back to Back, Back to Front and Front to Back. The distance between main and instrumental buildings are kept as 6m.

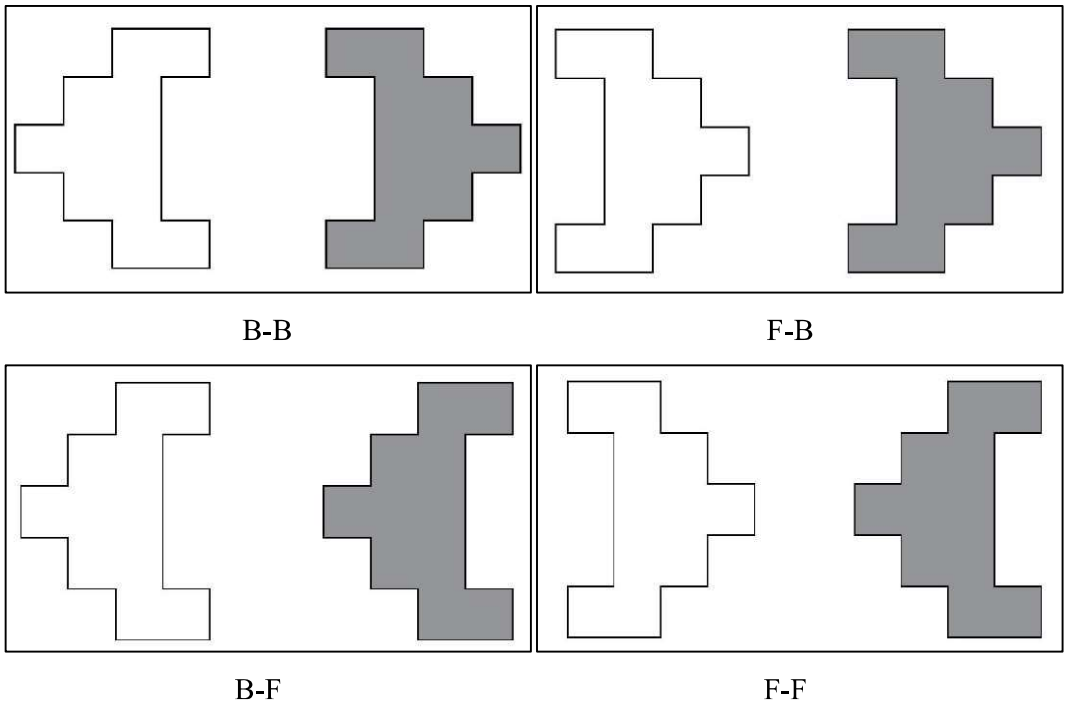

Fig 3.5 Interference conditions for S1

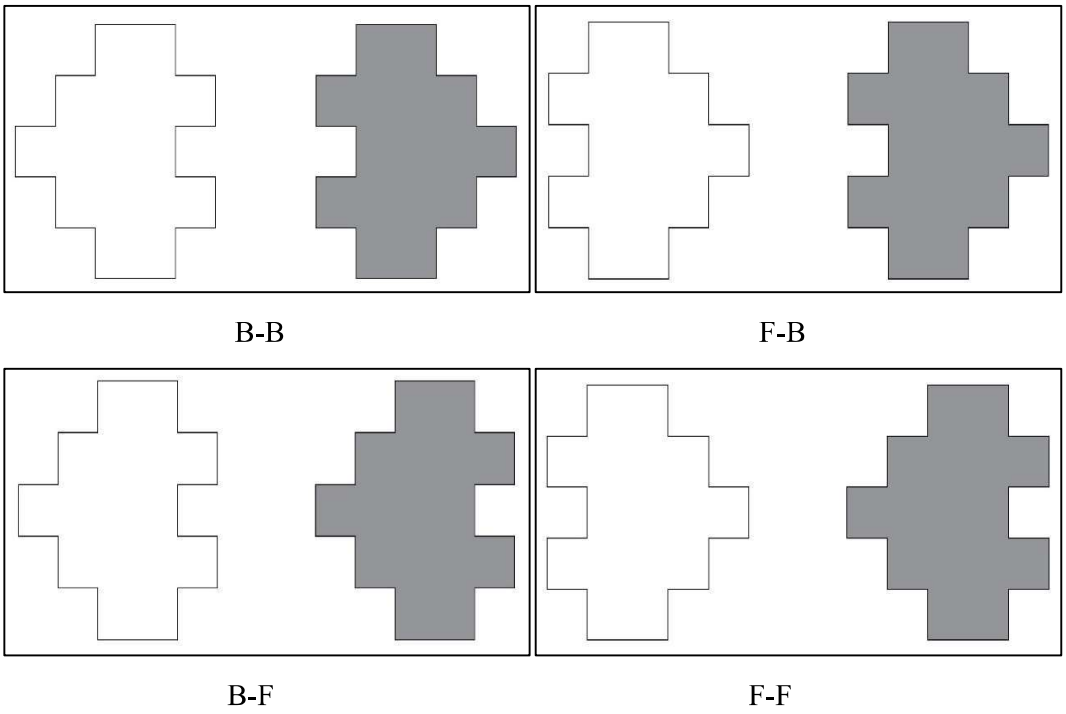

Fig 3.6 Interference conditions for S2

3.2.3 MESHING

Meshing is an important step in numerical simulation and a well properly meshed model results in most accurate results. Meshing includes significant flow aspects that are affected by flow factors, such as grid refinement within the wall boundary layer. Before meshing, each face of the building and domain is named as it is required for the application of flow physics. To achieve uniform flow around the model, tetrahedral meshing with inflation control was created. To keep the model's shape, the mesh size function is set to curvature. The mesh size can be varied to get the required number of nodes and elements. If the number of nodes and elements are kept low, the accuracy of the results will be reduced, whereas a higher node and element number will complicate the process of meshing. The different meshing adopted in this model are: building meshing, domain meshing and inflation. Inflation is for the proper capture of flow at the interface. The various meshing taken is shown in figures below:

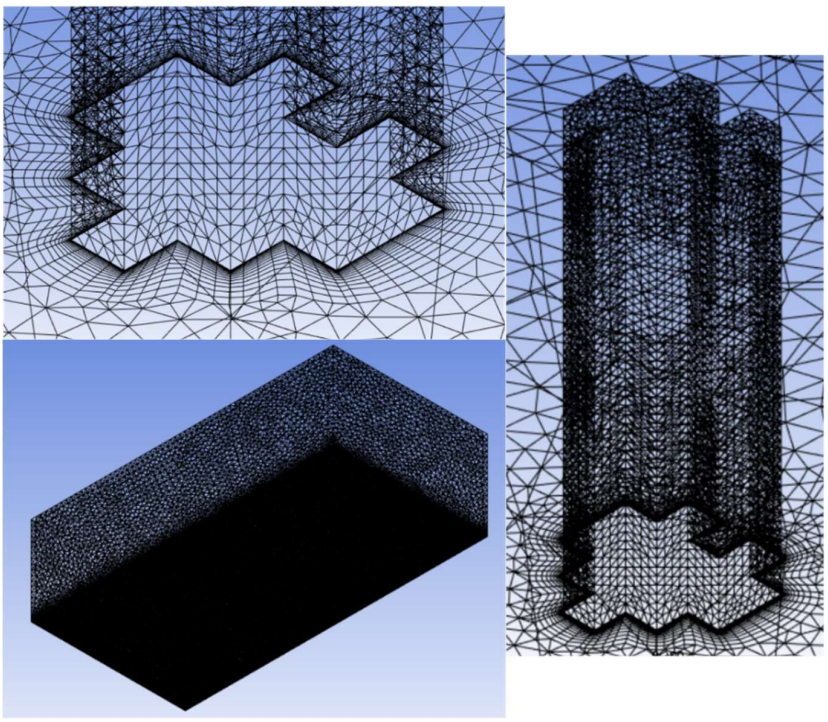

Fig 3.7. Meshing of model

The different mesh sizes adopted for the model is given in table below:

Table 3.1. Adopted mesh sizes

Criteria	Value
Face sizing	0.0125 m
Edge sizing	0.025 m
Ground sizing	0.05 m
Inflation layers	15
Domain sizing	0.2 m

The face and edge sizing are for the building, whereas ground sizing is for the ground surface of domain.

3.2.4 BOUNDARY CONDITIONS (Cfx-Pre)

The boundary conditions are assigned to have a link between actual and virtual wind tunnel. It is provided so as to give the natural wind condition inside the domain created in numerical simulation. The inlet velocity is provided using power law which is given in equation (3.13). The reference height taken here is 1m and the reference velocity taken is 10m/s. The value of 'α' is taken as 0.15. Also, the pressure at outlet is given as 0 Pa. In the next step, the ground surface of domain and the building faces were given no slip condition. The side and top wall of the domain is given free slip condition as no force is generated on it.

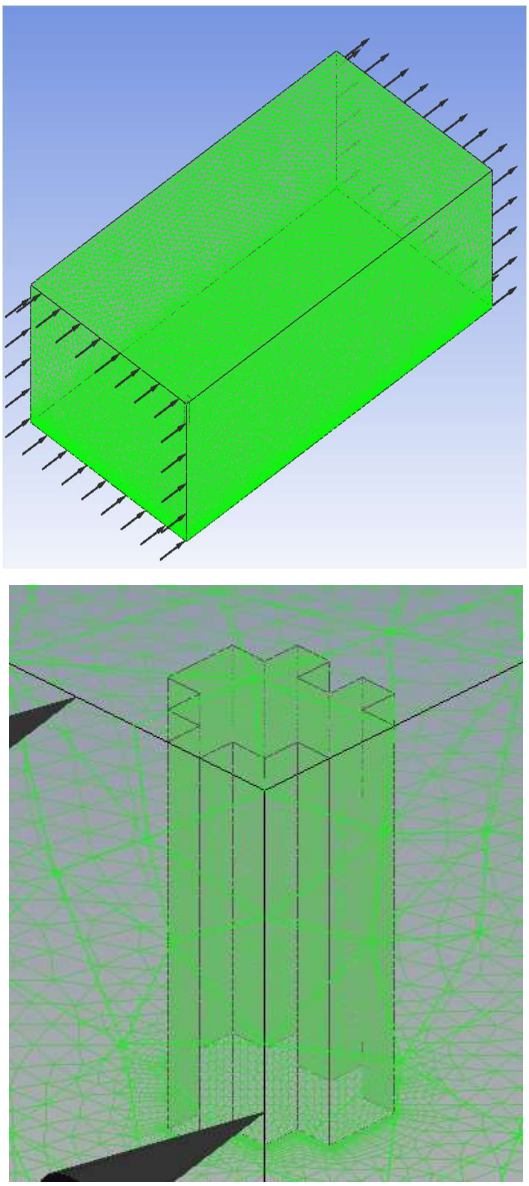

Fig 3.8. Model and domain after assigning boundary conditions

3.2.5 CFX-SOLVER

At this stage, the simulation is run and iterations are done. At the end of iterations graphs showing convergence of several factors has been obtained.

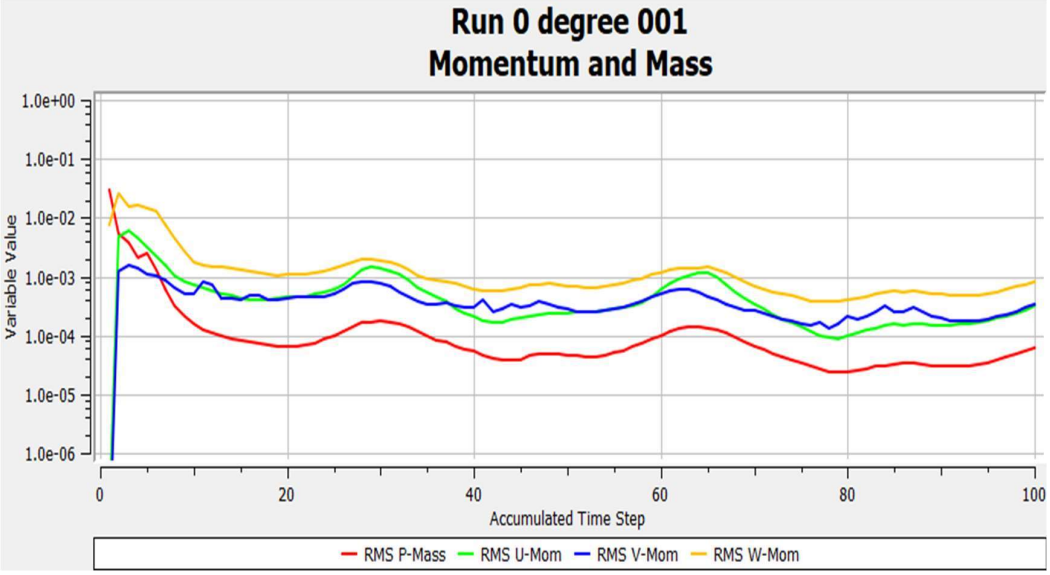

Fig 3.9. Convergence of momentum and mass

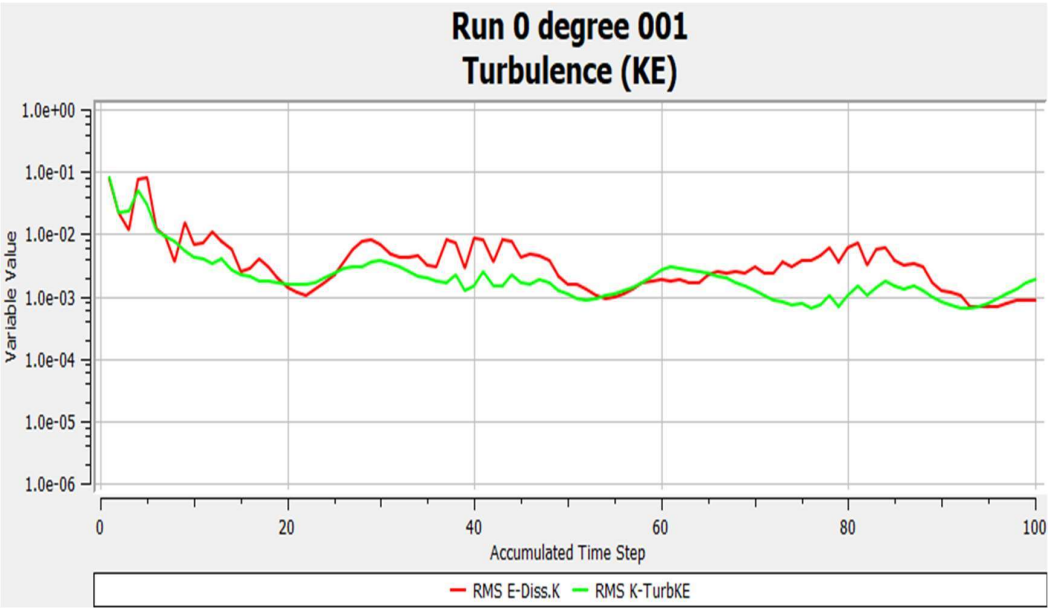

Fig 3.10. Convergence of kinetic energy

3.2.5 CFD-POST

The various wind effects are obtained in graphical form after the simulation. The pressure distribution along the building face can be obtained in form of pressure contours. The

effect of building on the wind flow pattern can be determined from the velocity streamlines. The coefficient of pressure (C_p) for each face can be obtained with the help of vertical lines drawn on every face. The various points in the line act as pressure points and it gives the pressure variation along the height. The lines are drawn on models as shown in figure below:

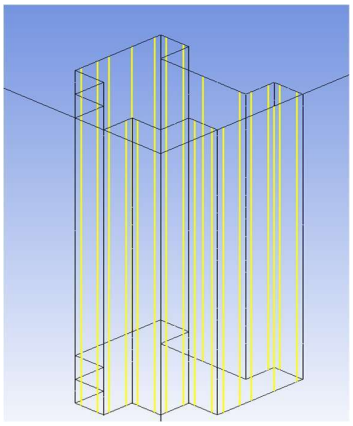

Fig 3.11 Lines drawn to extract pressure values

The pressure data is exported to excel and the coefficient of pressure is obtained using the equation,

$$C_p = \frac{P}{0.5*\rho*V^2} \tag{3.16}$$

where,

P – pressure

ρ – density of air (1.225kg/m^3)

V – velocity (10 m/s)

The forces along x and z directions are also found using the equation,

$$C_{f_x} = \frac{f_x}{0.5*\rho*V^2*L_z*H} \tag{3.17}$$

$$C_{f_z} = \frac{f_z}{0.5*\rho*V^2*L_x*H} \tag{3.18}$$

3.3 VALIDATION

The validation is done on a rectangular or square model without any corner cuts or any other configurations. The standards and codes are always based on conventional regular models, hence its always easy to do validation with the help of such models. A square

model of dimension 200mm x 200mm is taken, so as to make the cross-sectional area same as that of the models taken. The height of the square model is also taken as 600mm. The square model undergoes every procedure in the simulation and the coefficient of pressure (C_p) value is found. It is then compared with the C_p value of square models mentioned in IS 875 (part 3): 2015. The values were in good agreement and the same parameters are used for the simulation of the study models. The square model which is used for the simulation is shown below:

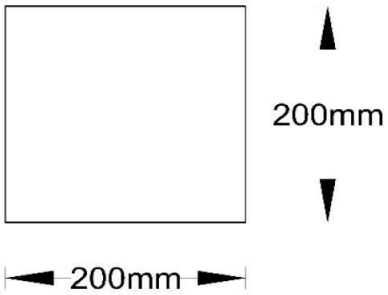

Fig 3.12. Square model for validation

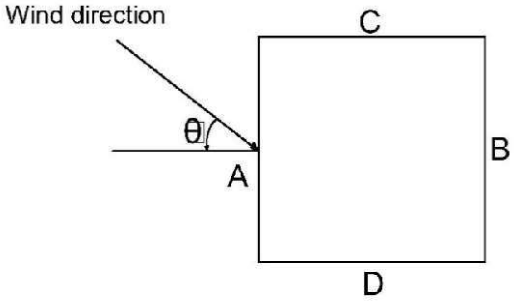

Fig 3.13. Naming of the model according to code

Table 3.2. Validation of obtained value with IS:875 (Part III)- 2015

C_p at 0°	Faces of square model			
	A	B	C	D
IS:875 (Part III)-2015	+0.8	-0.25	-0.8	-0.8
Square Model	+0.75961	-0.27062	-0.73655	-0.73655

CHAPTER 4

RESULTS AND DISCUSSIONS

4.1 GENERAL

Fish shaped models 1 and 2 are analysed both in isolated condition and under the effect of interference. The presence of an adjacent building results in change in the response of buildings under wind action. This chapter discusses results of both the models, so as to determine the performance of buildings under the action of wind. The variation of Cp at every face of the model at different wind incidence angle, pressure contours for both the models under isolated conditions, horizontal streamlines, comparison of Cp of model under isolated and grouped condition and drag force coefficients of model under isolated condition are discussed in this chapter.

The faces of the models are named at the meshing stage and in this study the faces are named as shown below:

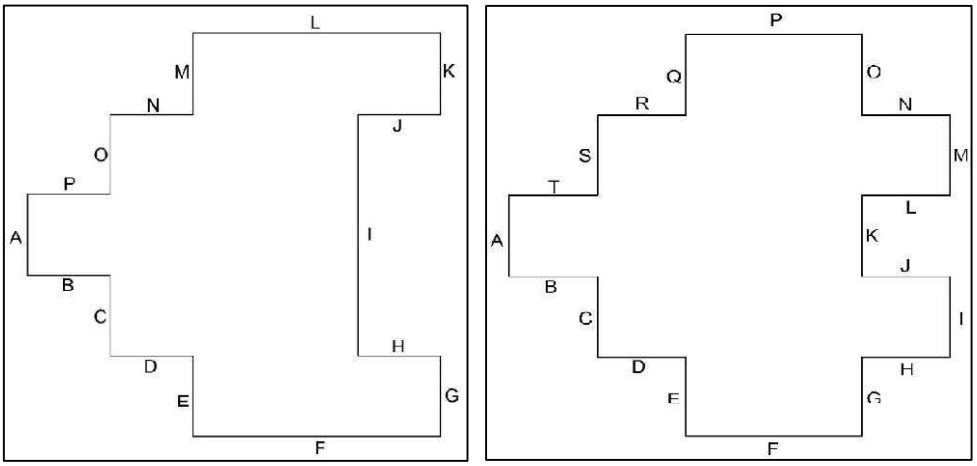

Fig 4.1. Naming of faces of S1 and S2

4.1.1 VARIATION OF C_p AT DIFFERENT WIND INCIDENCE ANGLE

Coefficient of pressure is an important parameter to be considered while analysing a building under the effect of wind. This factor is taken into consideration when the air

infiltration rate of a building has to be determined. According to IS 875 (Part 3): 2015, the wind load functioning normally on a surface is calculated by multiplying the total area of the surface, or an appropriate portion of it, by the pressure coefficient and the design wind pressure at the surface's height above the ground. Figure depicts the variation of the coefficient of pressure with changing wind incidence angle.

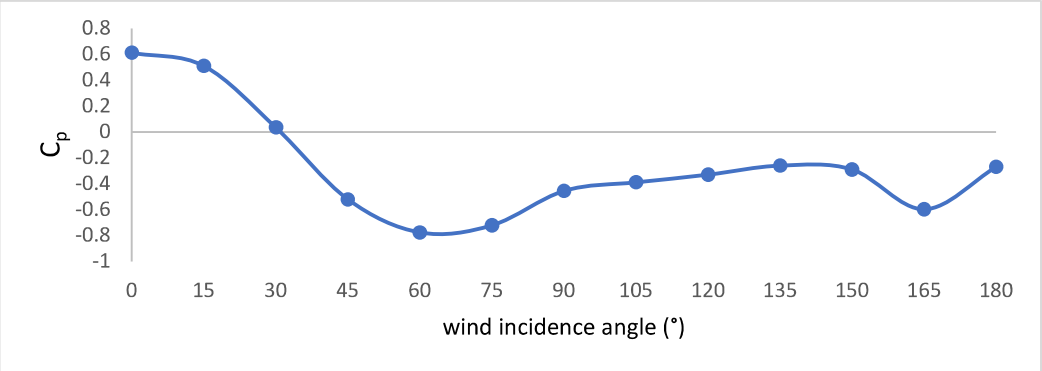

Fig 4.2. Variation of C_p for face A of S1

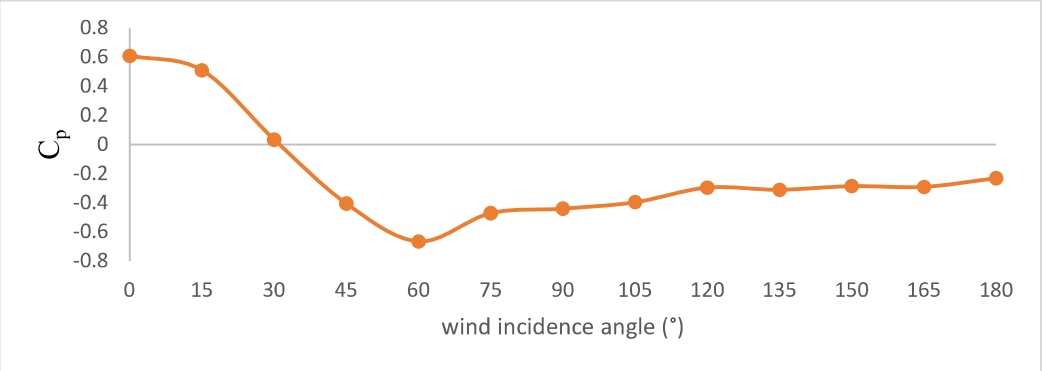

Fig 4.3. Variation of C_p for face A of S2

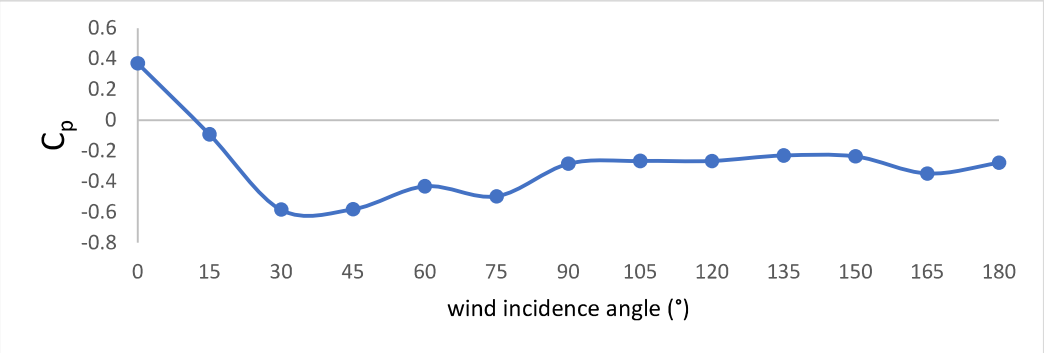

Fig 4.4. Variation of C_p for face B of S1

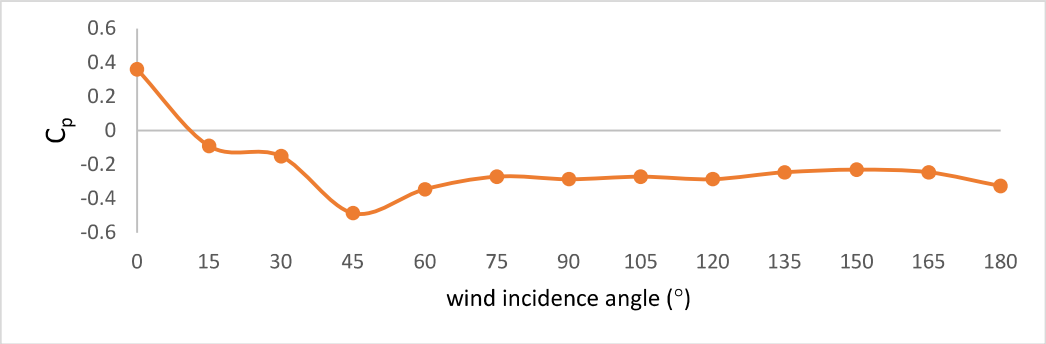

Fig 4.5. Variation of C_p for face B of S2

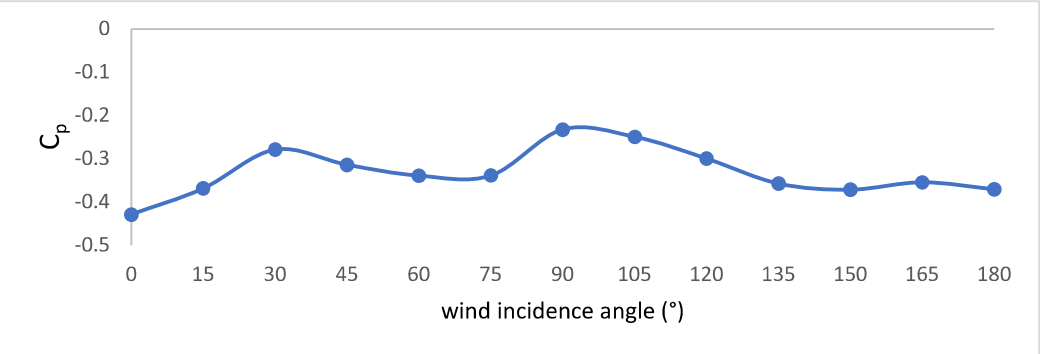

Fig 4.6. Variation of C_p for face F of S1

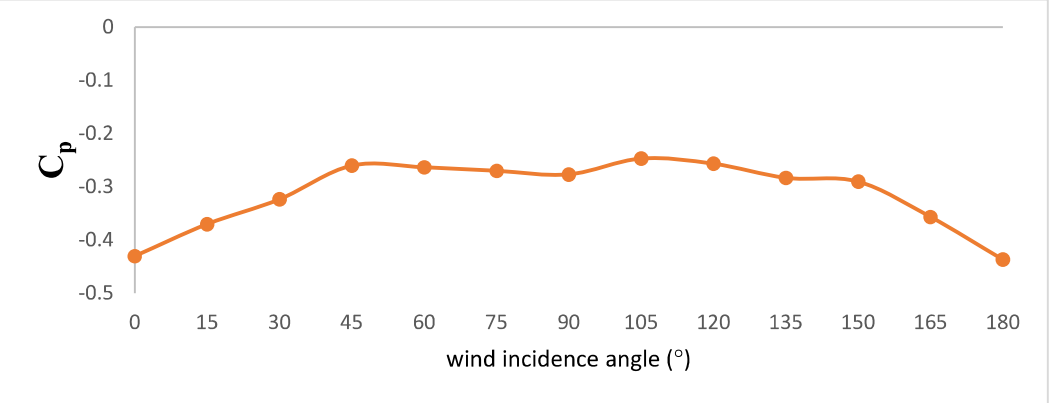

Fig 4.7. Variation of C_p for face F of S2

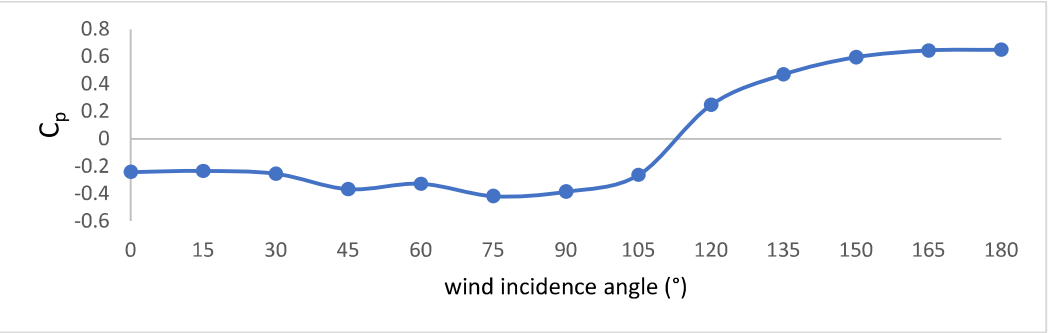

Fig 4.8. Variation of C_p for face I of S1

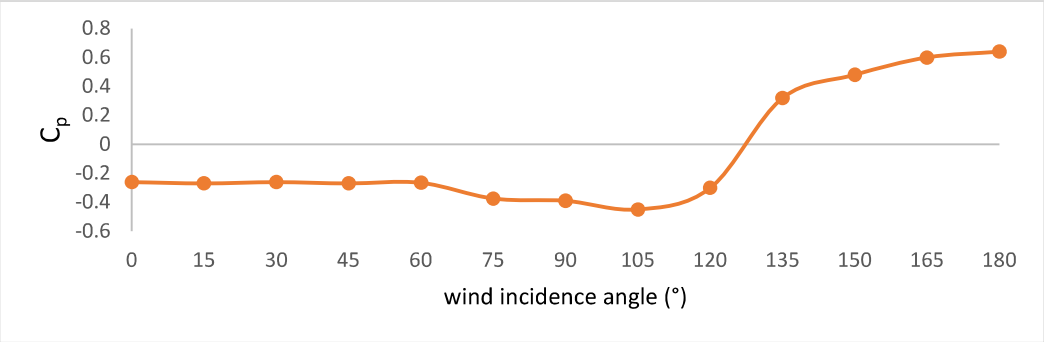

Fig 4.9. Variation of C_p for face K of S2

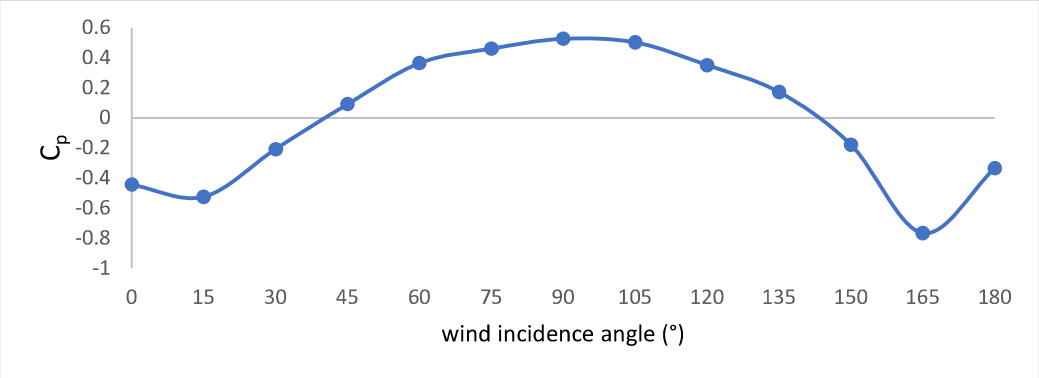

Fig 4.10. Variation of C_p for face L of S1

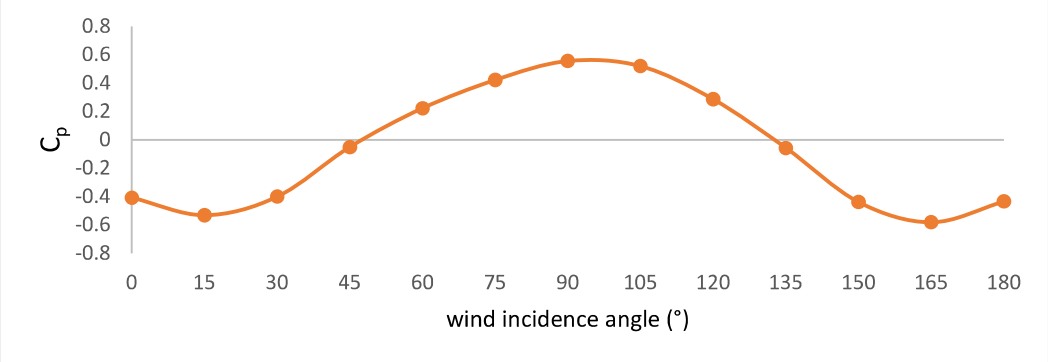

Fig 4.11. Variation of C_p for face P of S2

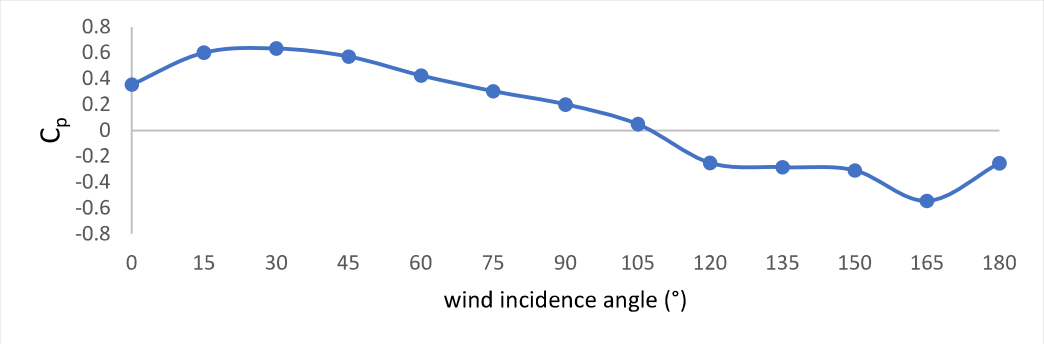

Fig 4.12. Variation of C_p for face P of S1

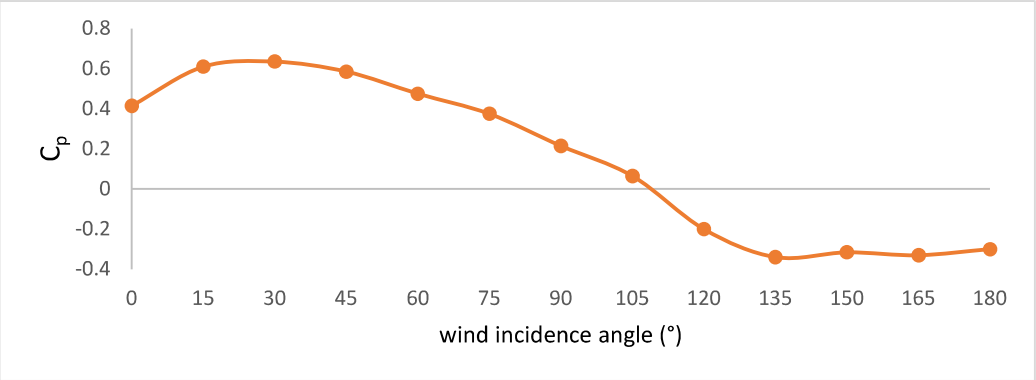

Fig 4.13. Variation of C_p for face T of S2

The C_p vs angle graph shows the variation of pressure coefficient at different wind incidence angles. The graphs for both the models are plotted and it is observed that the variation is almost similar in both the cases. The main difference is observed because of the extra corner cut provided in the second model. Taking the first model (S1), it is observed that the maximum coefficient value **0.65** is obtained on **face I** at an angle of **180°** and the minimum value **-0.78** is observed on **face A** at an angle of **60°**. Whereas in case of second model (S2), the maximum value **0.65** is obtained on **face N** at **135°** and minimum value **-0.77** on **face M** at **105°.** Analysing the maximum value, it is clear that the maximum value is obtained when the face is exactly perpendicular to the wind direction and on the windward side. Taking the variation of C_p for face A for both the model, the variation is quite similar in both the cases. The Cp value changes from positive to negative due to suction. In both the models, face F is where flow separation and vortex formation occur, as a result of which the face experiences suction at every angles. Considering the leeward face of both the models, face I of model 1 and face K of model 2 a similar variation is seen. This is because, at 0°, both the faces are at leeward side where the faces experiences suction, hence a negative C_p. At 180°, both the faces come at the wind ward side, where it has the maximum positive C_p. Similarly, the variation is same in the case of face L of S1 and face P of S2. Face P of S1 and face T of S2 shows similar variation.

4.1.2 PRESSURE CONTOURS

Pressure contour for a building face shows the variation of pressure along the building height in form of contours. It is obtained according to width and height of a building face. Both the models are having corner cuts and contours corresponding to each wind incidence angle is shown. For faces on windward side, positive pressure is observed and it changes according the face location. The wind angle is considered from 0°-180° and an interval of 15° is taken. The contours for 0°, 45°, 90°, 135° and 180° are presented here.

4.1.2.1 PRESSURE CONTOURS FOR S1

The pressure contour for S1 is shown below:

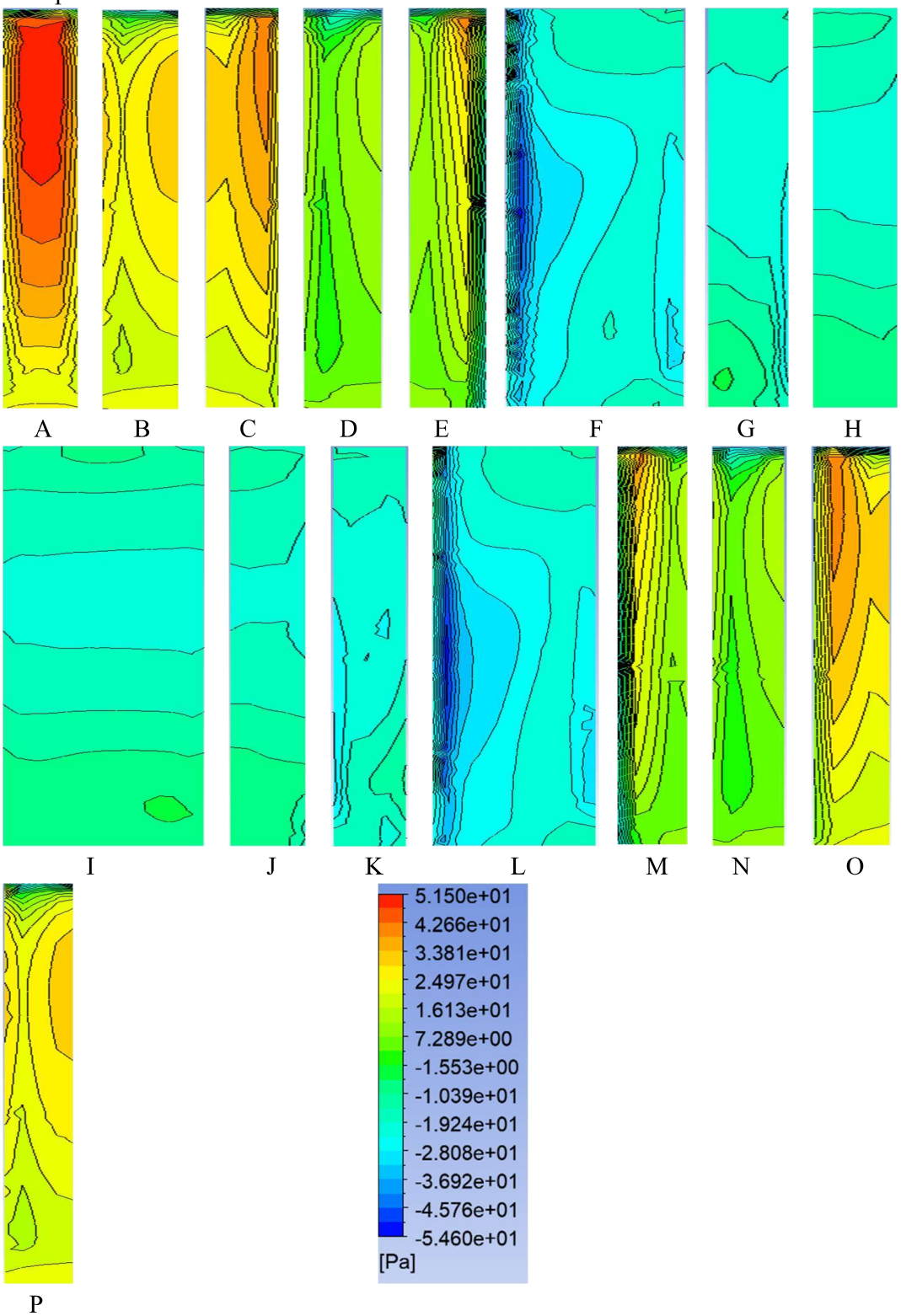

Fig 4.14. Pressure contour for S1 at 0°

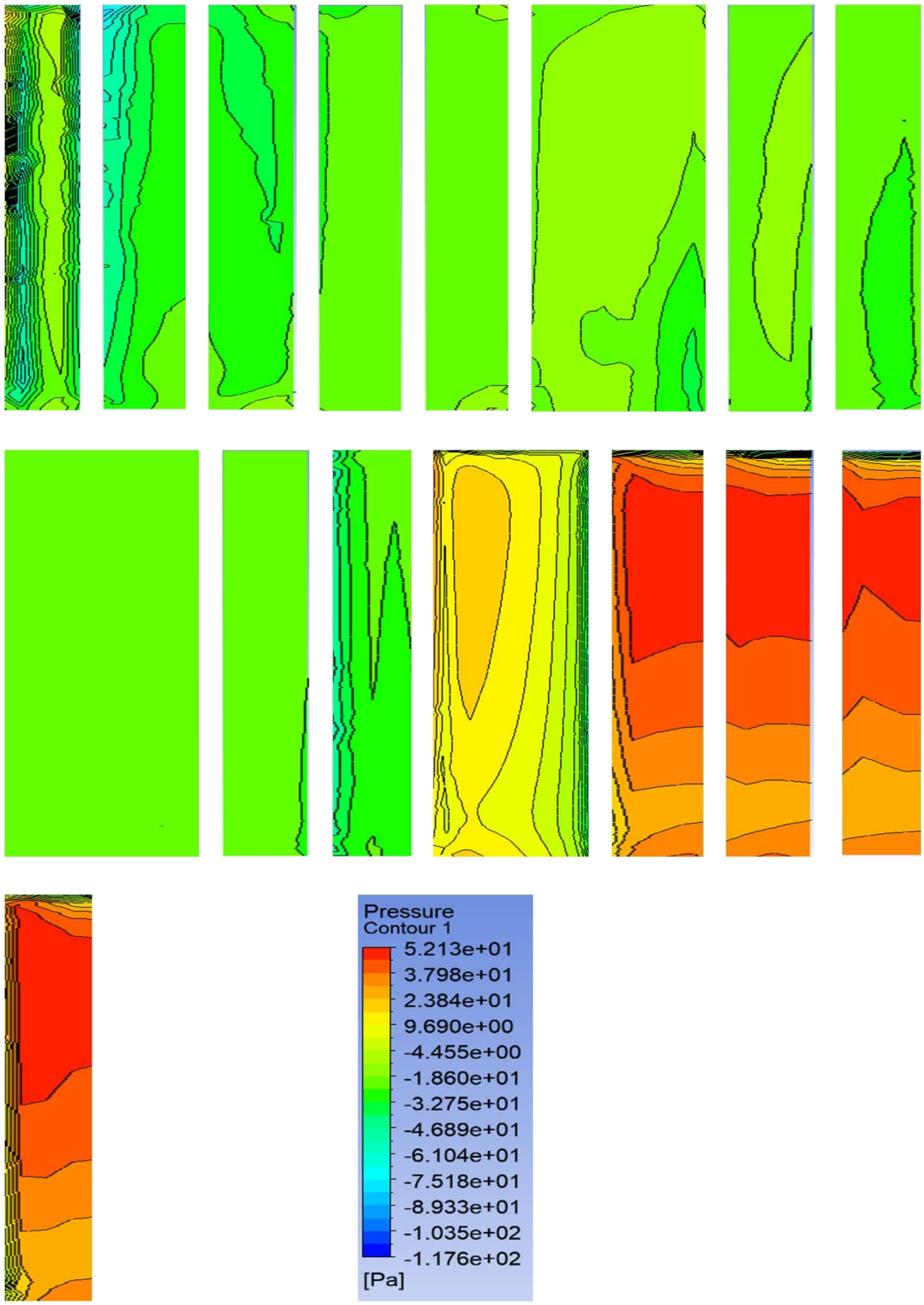

Fig 4.15. Pressure contour for S1 at 45°

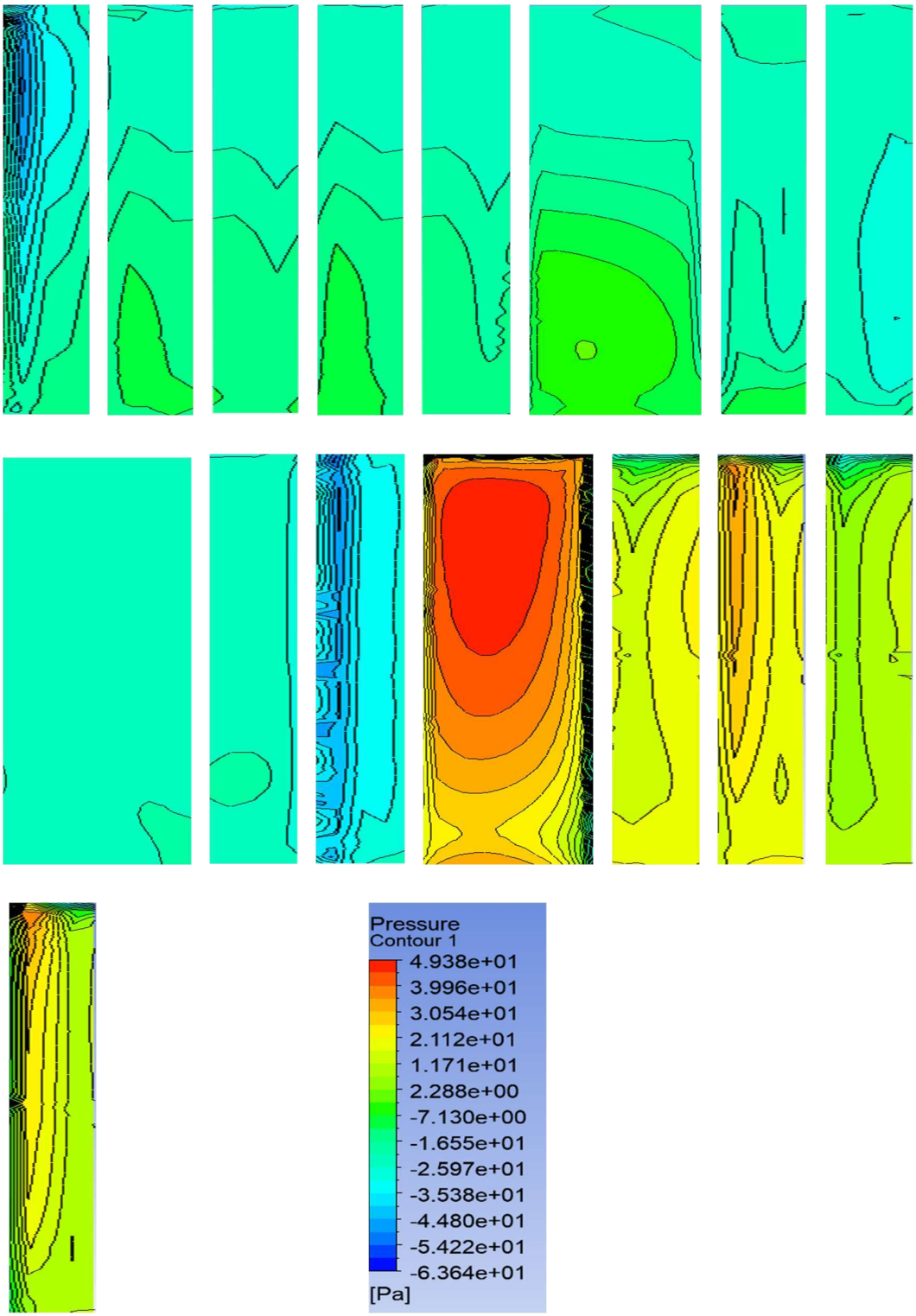

Fig 4.16. Pressure contour for S1 at 90°

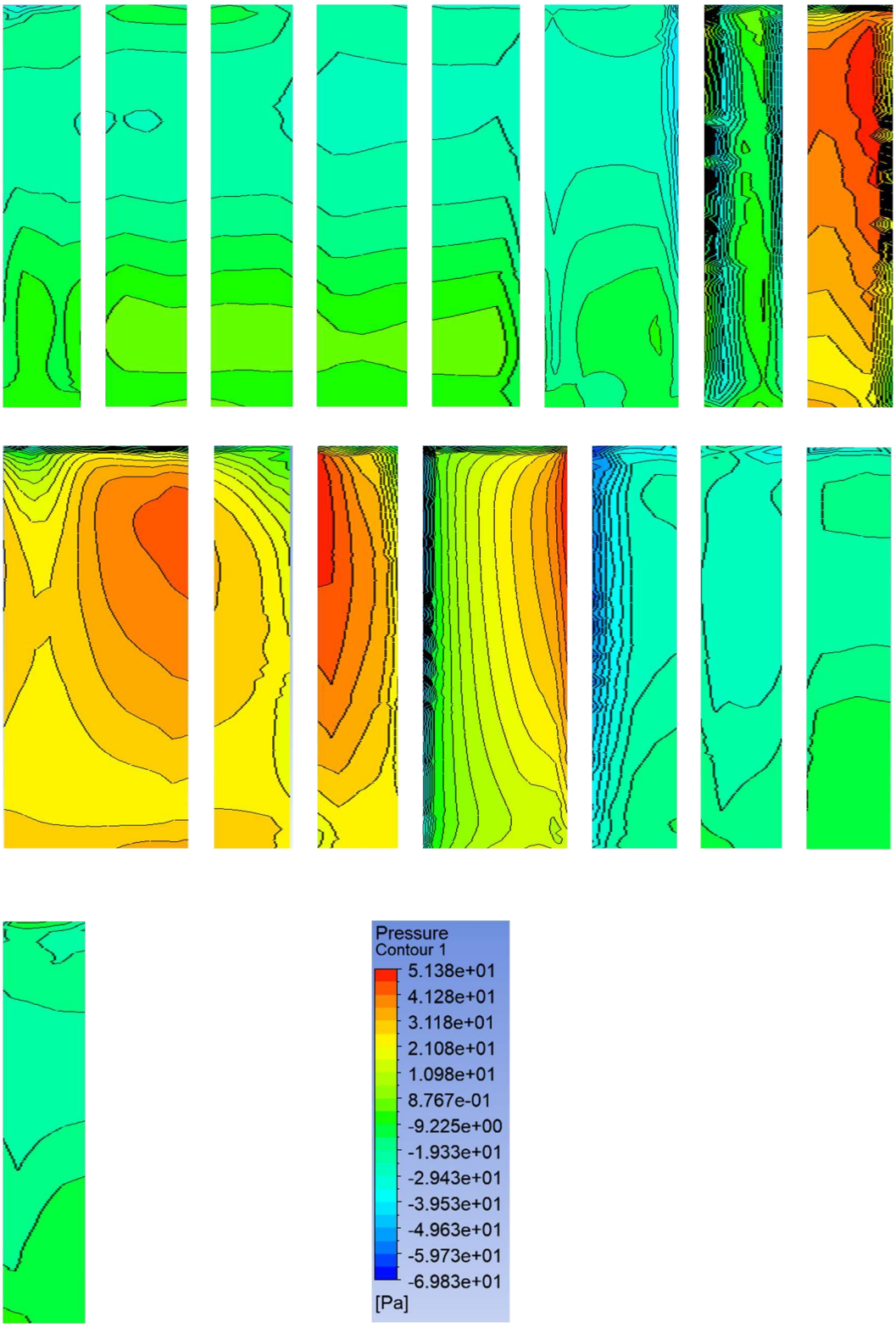

Fig 4.17. Pressure contour for S1 at 135°

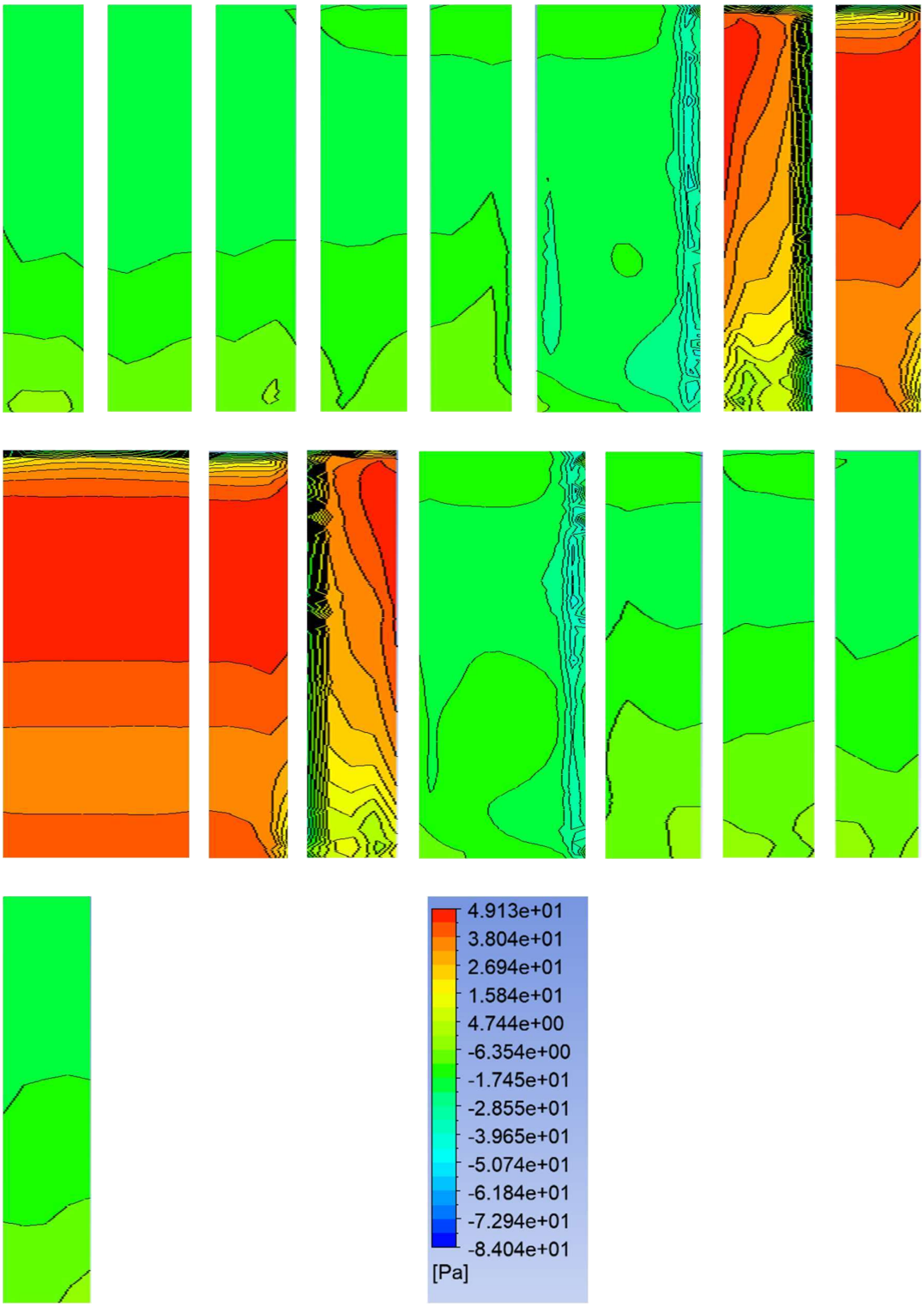

Fig 4.18. Pressure contour for S1 at 180°

It is clear from the pressure contour that the variation of pressure is unpredictable throughout the building height. Taking the case of contours at 0°, it is clear that positive pressure dominates on face A as the wind impinges on it directly. Considering the distribution of pressure along the height of face A, the pressure increaes with height. Since

the shape is symmetric, the faces on the opposite side shows almost the same contours. At face F and face L, suction dominates as it is the point of flow seperation and recirculation. At 180°, face I experiences very high pressure throughout its length, as it comes on the windward side.

4.1.2.2 PRESSURE CONTOURS FOR S2

Pressure contour for S2 is given below:

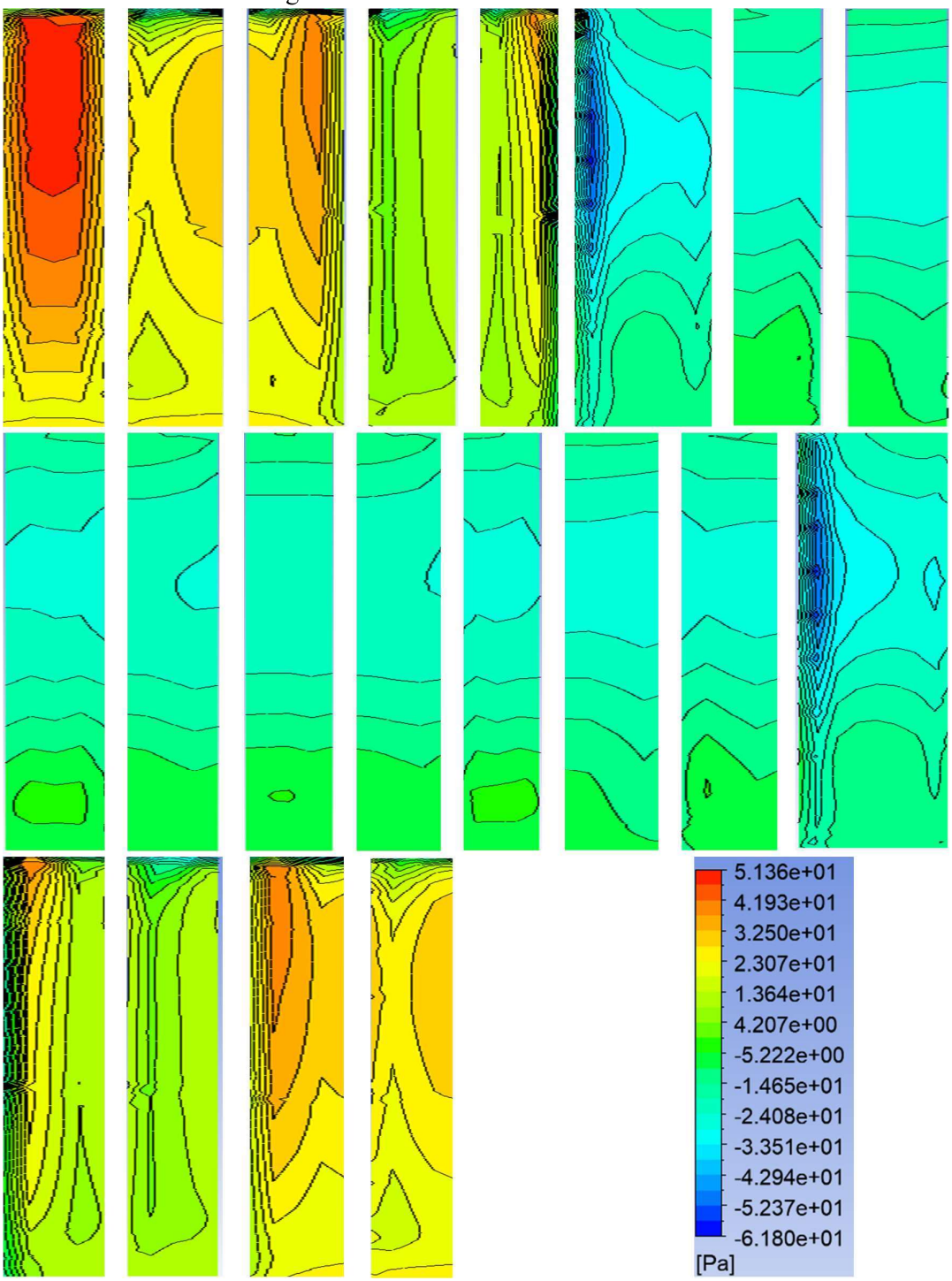

Fig 4.19. Pressure contour for S2 at 0°

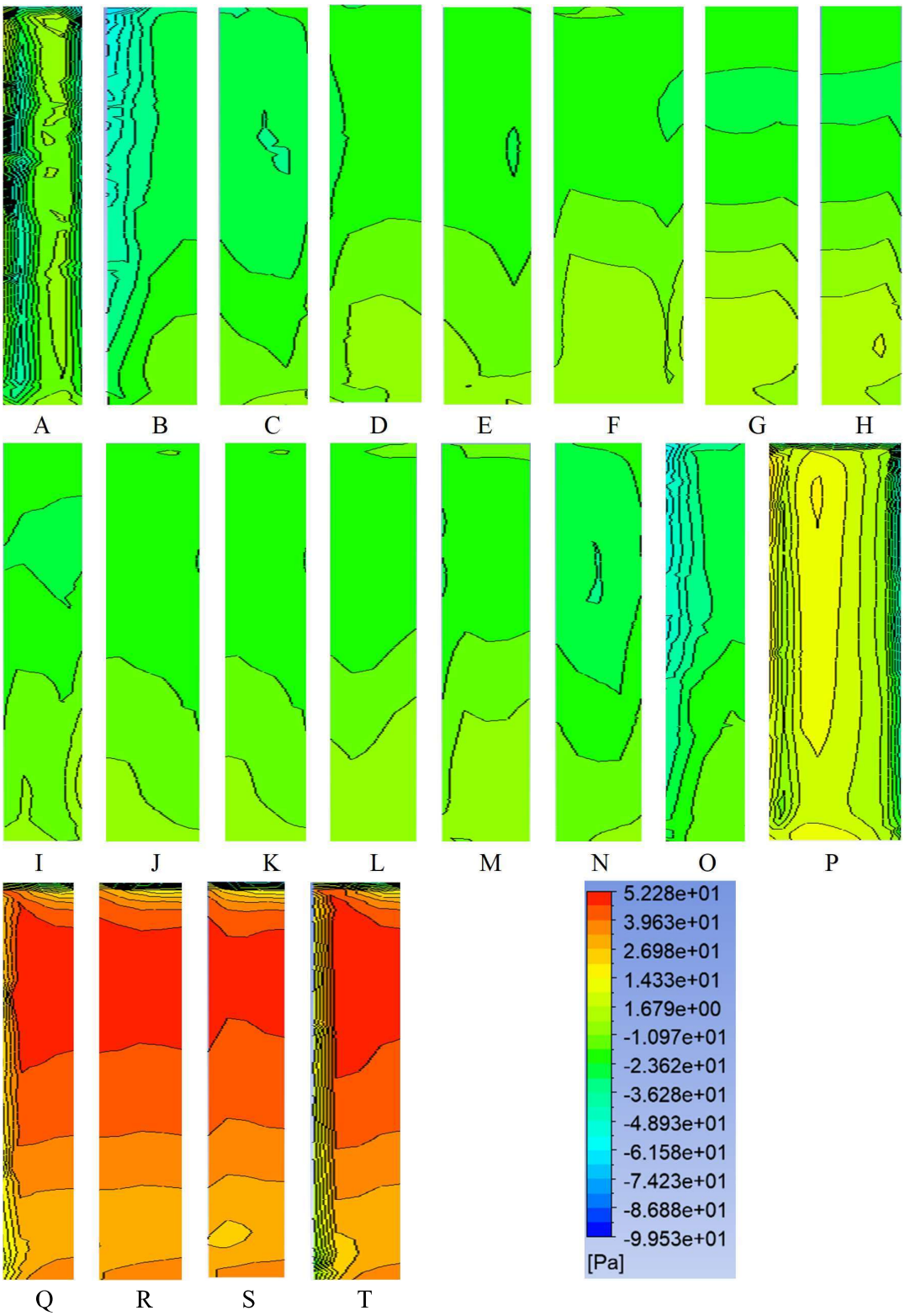

Fig 4.20. Pressure contour for S2 at 45°

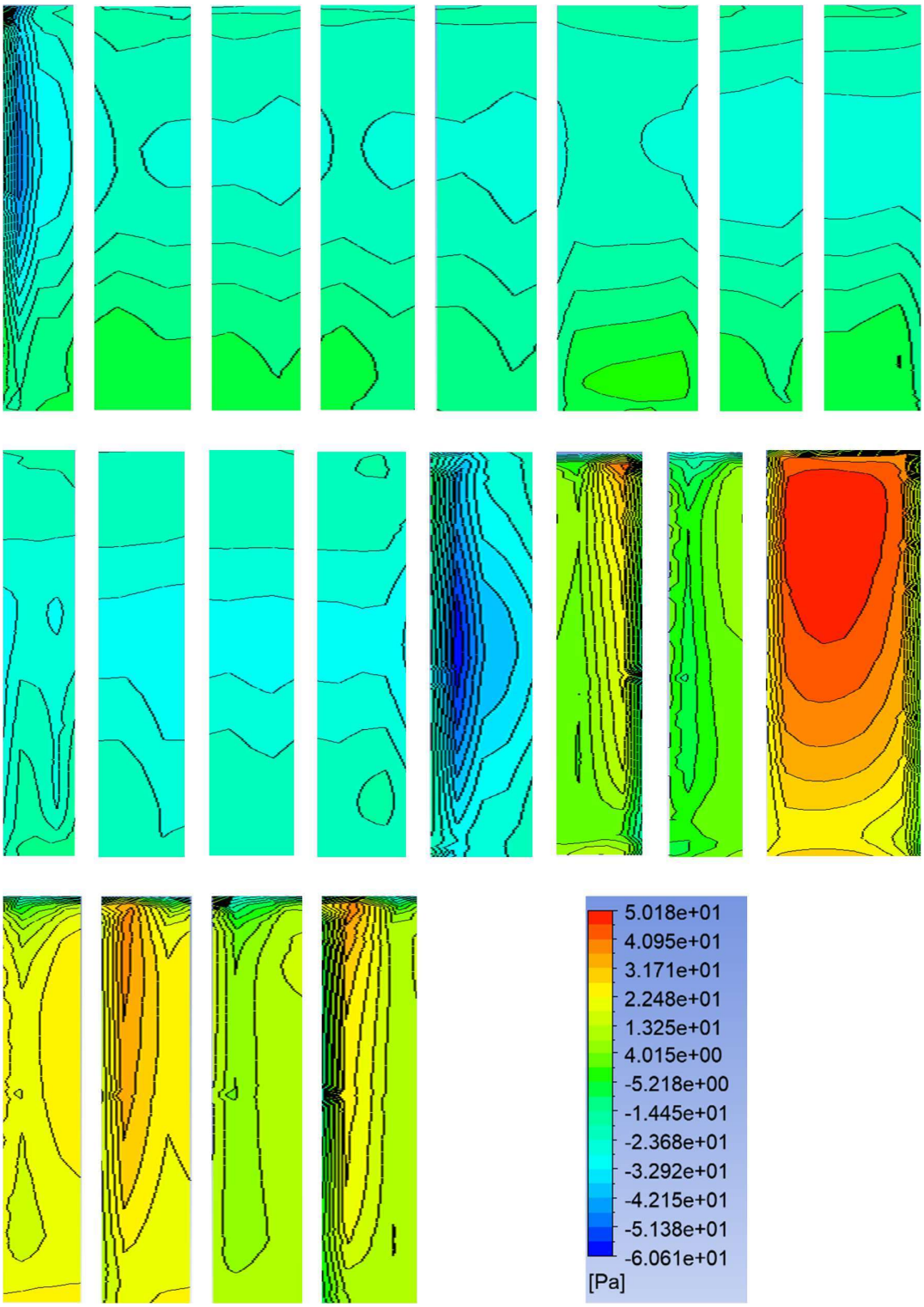

Fig 4.21. Pressure contour for S2 at 90°

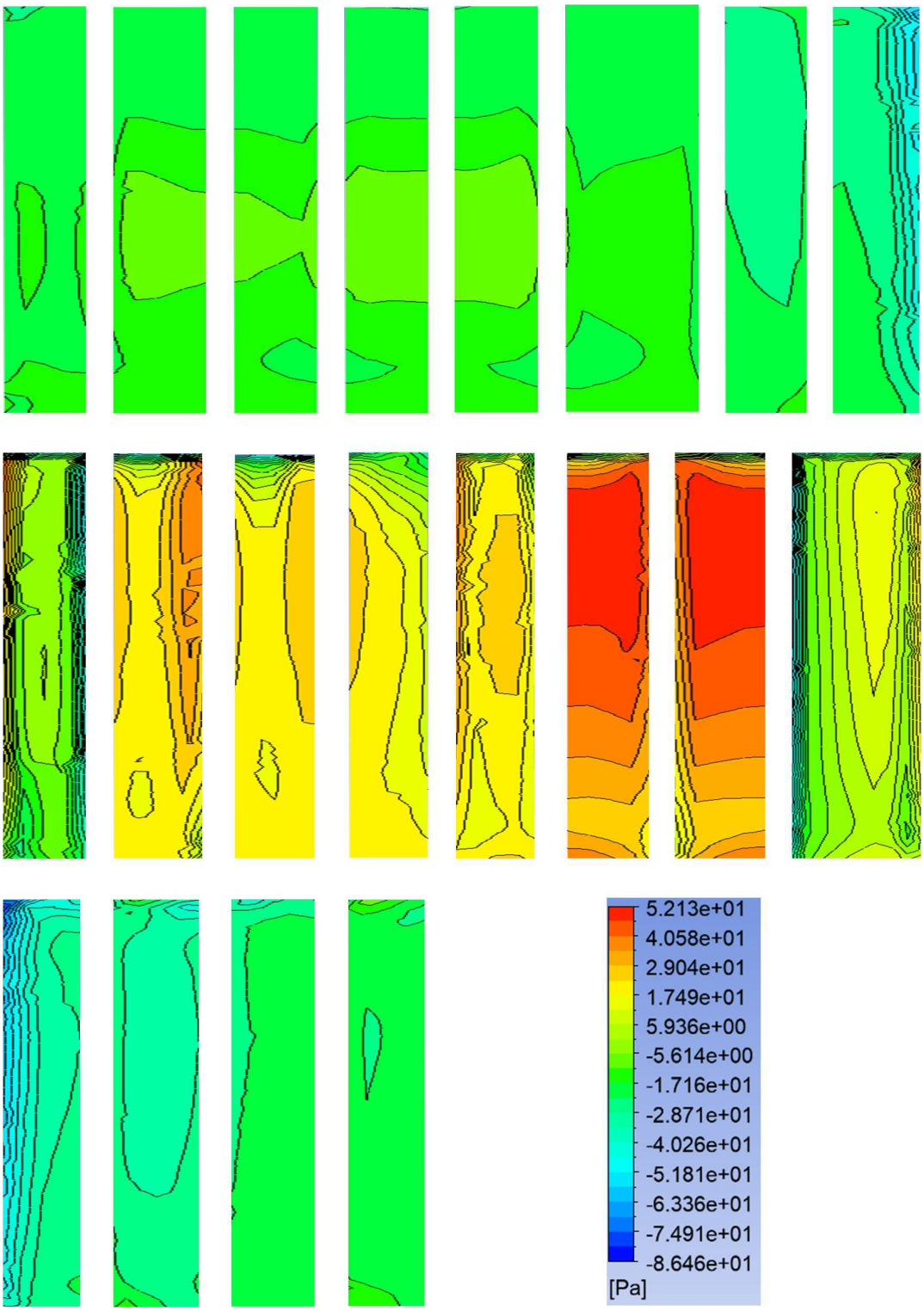

Fig 4.22. Pressure contour for S2 at 135°

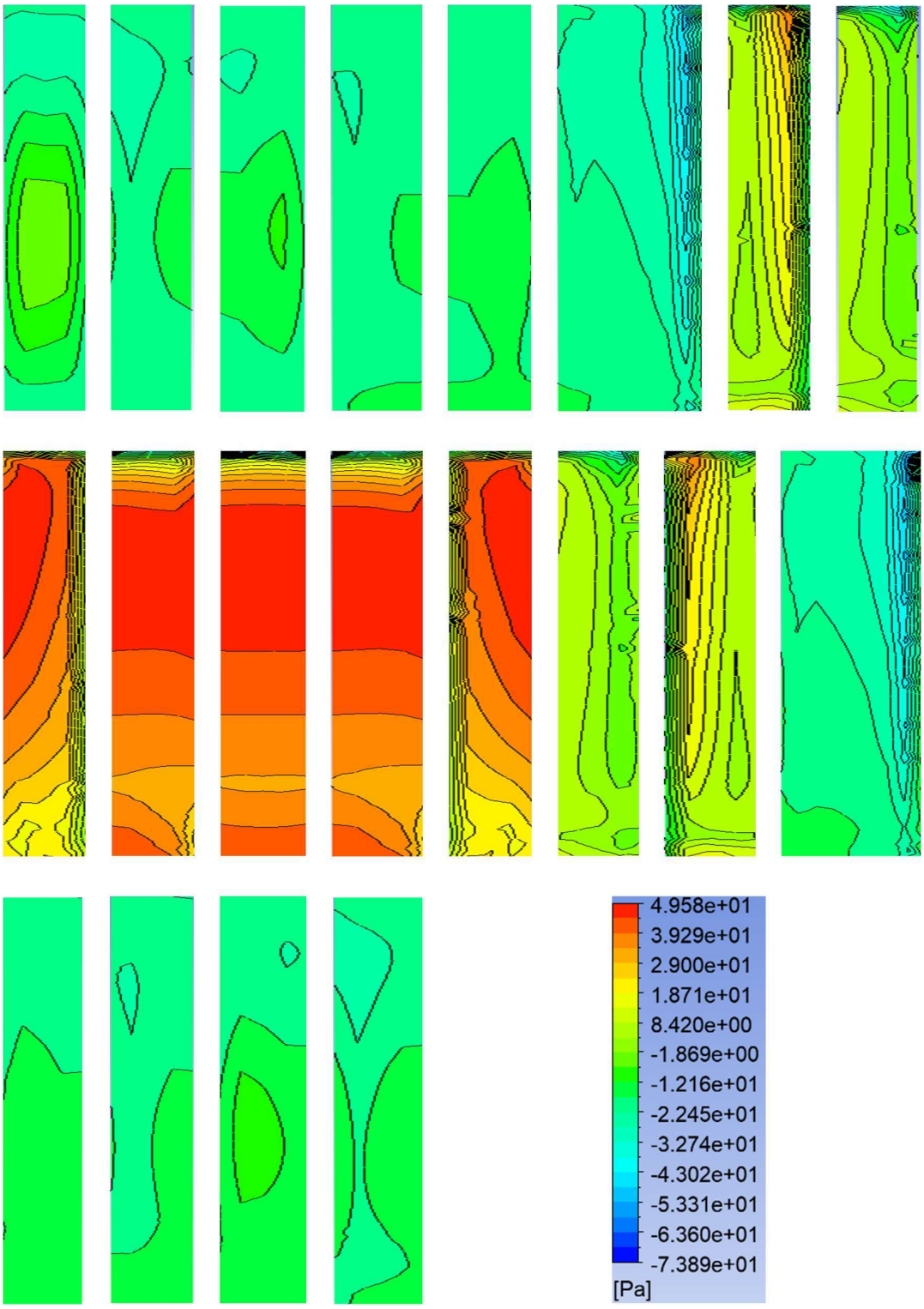

Fig 4.23. Pressure contour for S2 at 180°

The pressure distribution on different face of S2 at different wind incidence angle is shown above. At 90°, suction predominates and positive pressure can be seen only on few faces. The distribution is similar to that of S1, but the observed change is due to the presence of extra corner cuts which influences the wind flow. As discussed for S1,

positive pressure is seen on windward faces at 0° and the faces at back experience positive pressure at an angle of 180°.

4.1.3 HORIZONTAL STREAMLINES

A streamline is an imaginary line in the fluid whose tangent at any location depicts the direction of a fluid particle's velocity at that position.The wind flow streamlines are obtained for both the models S1 and S2 at all the wind incidence angle. The streamline shows the flow of wind, the seperation of flow, formation of voterx and recirculation zone. The streamlines for both the models are taken at a height of 300mm.

4.1.3.1 STREAMLINES FOR S1

The streamlines for model 1 for every wind incidence angle is shown below:

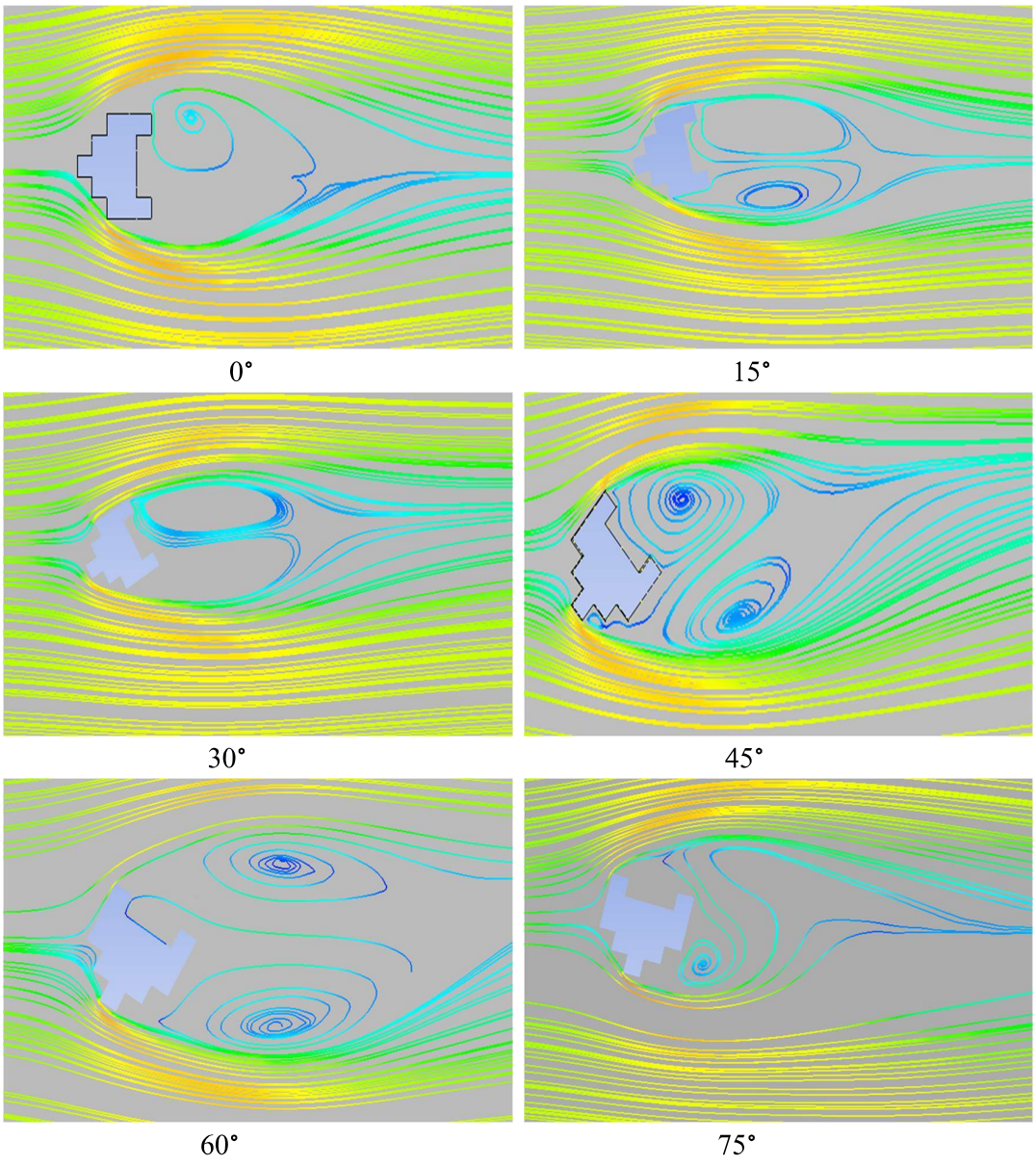

0° 15°

30° 45°

60° 75°

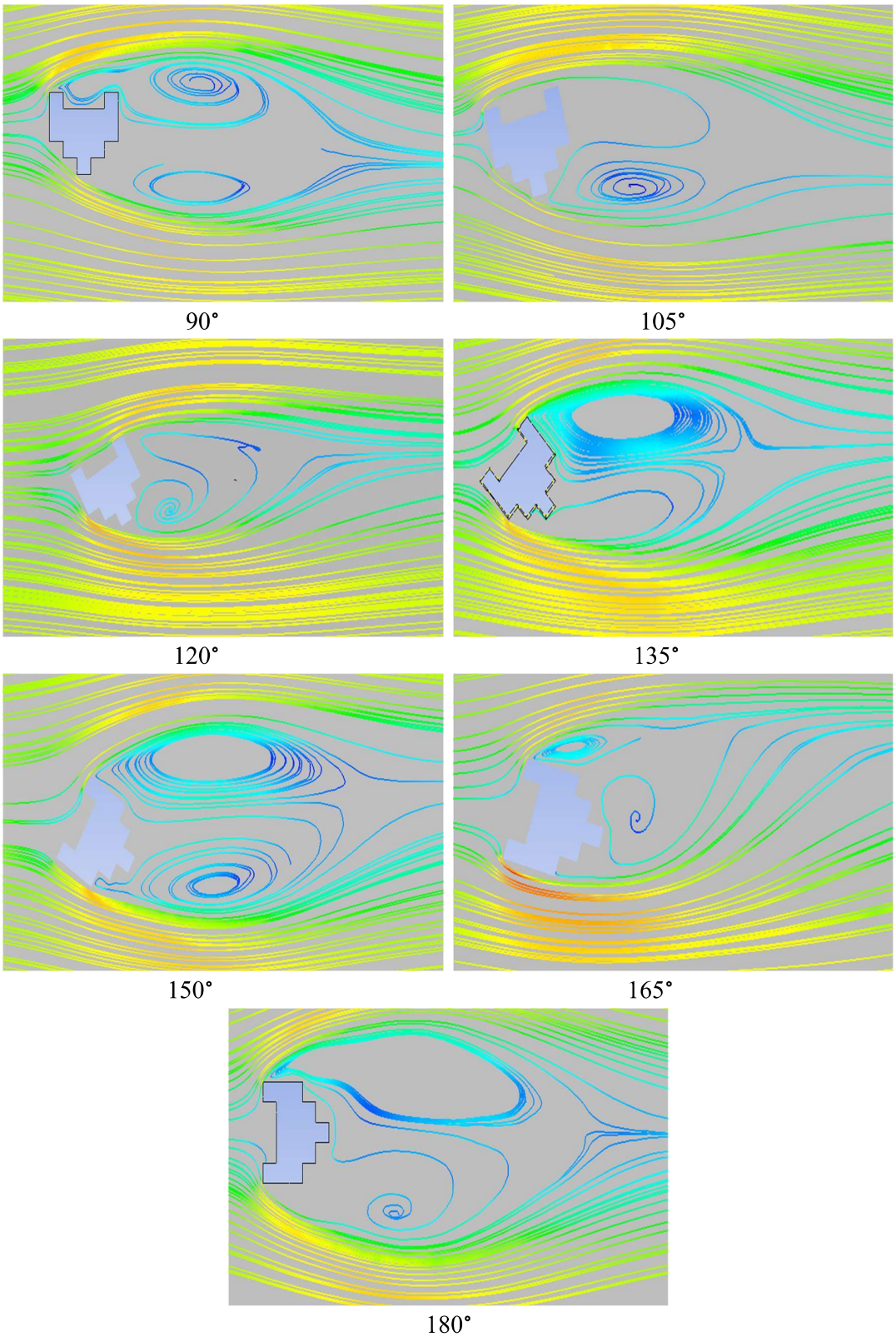

Fig 4.24. Velocity streamlines for S1 at different wind incidence angle

Symmetrical flow lines in case of S1 is observed in case of 60° and 150°, which indicates less turbulence at this angle of incidence. The effect of vortex shedding is least observed in these cases. The pattern in which the wind flow recirculates and separate is not same for all the faces along flow direction due to the gustiness and turbulence of the flowing wind. Flow separation occurs at the edge of the faces and vortex are formed at the rear side of the building, resulting in suction at that region.

4.1.3.2 STREAMLINES FOR S2

The following are the streamlines observed for S2:

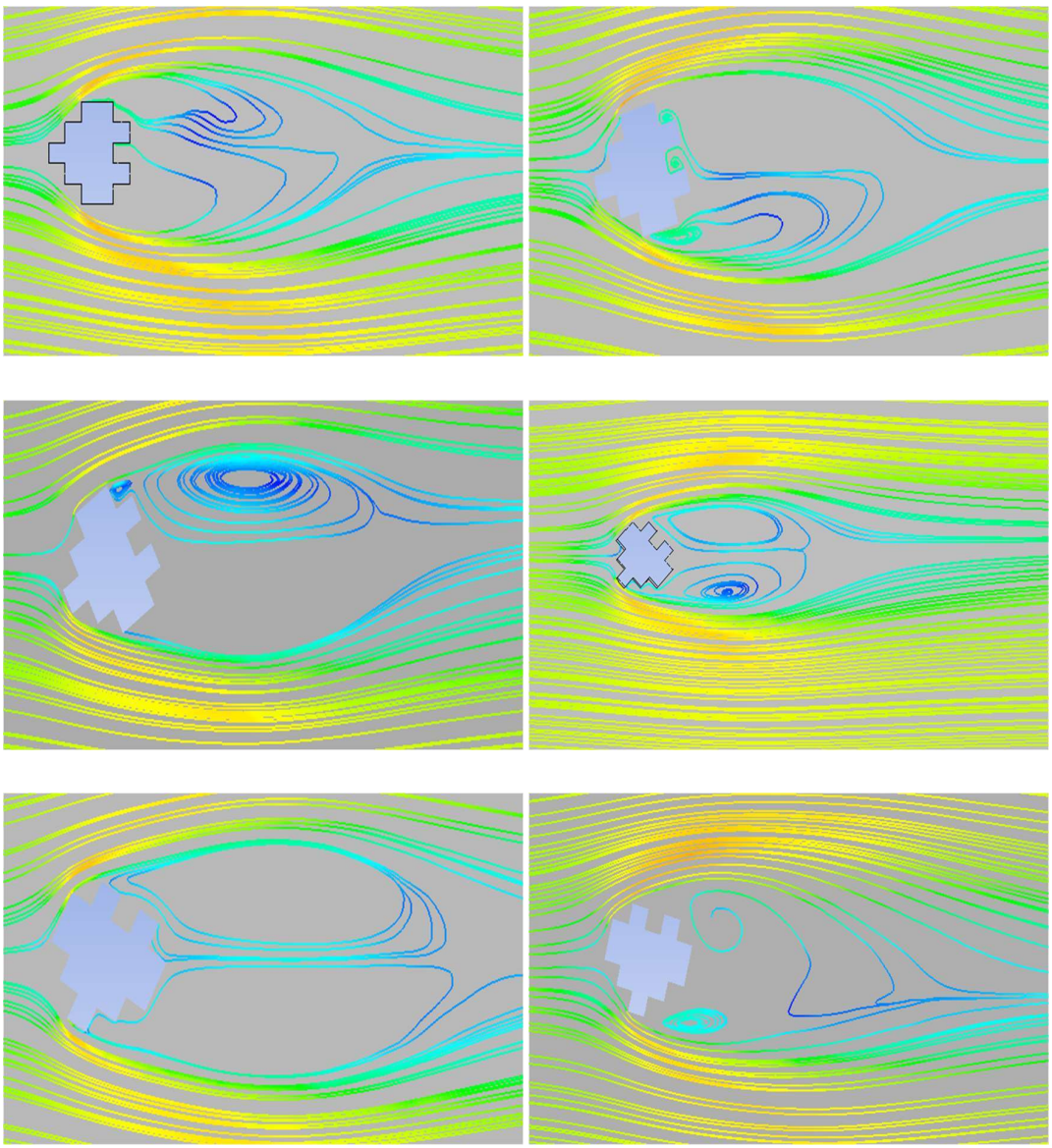

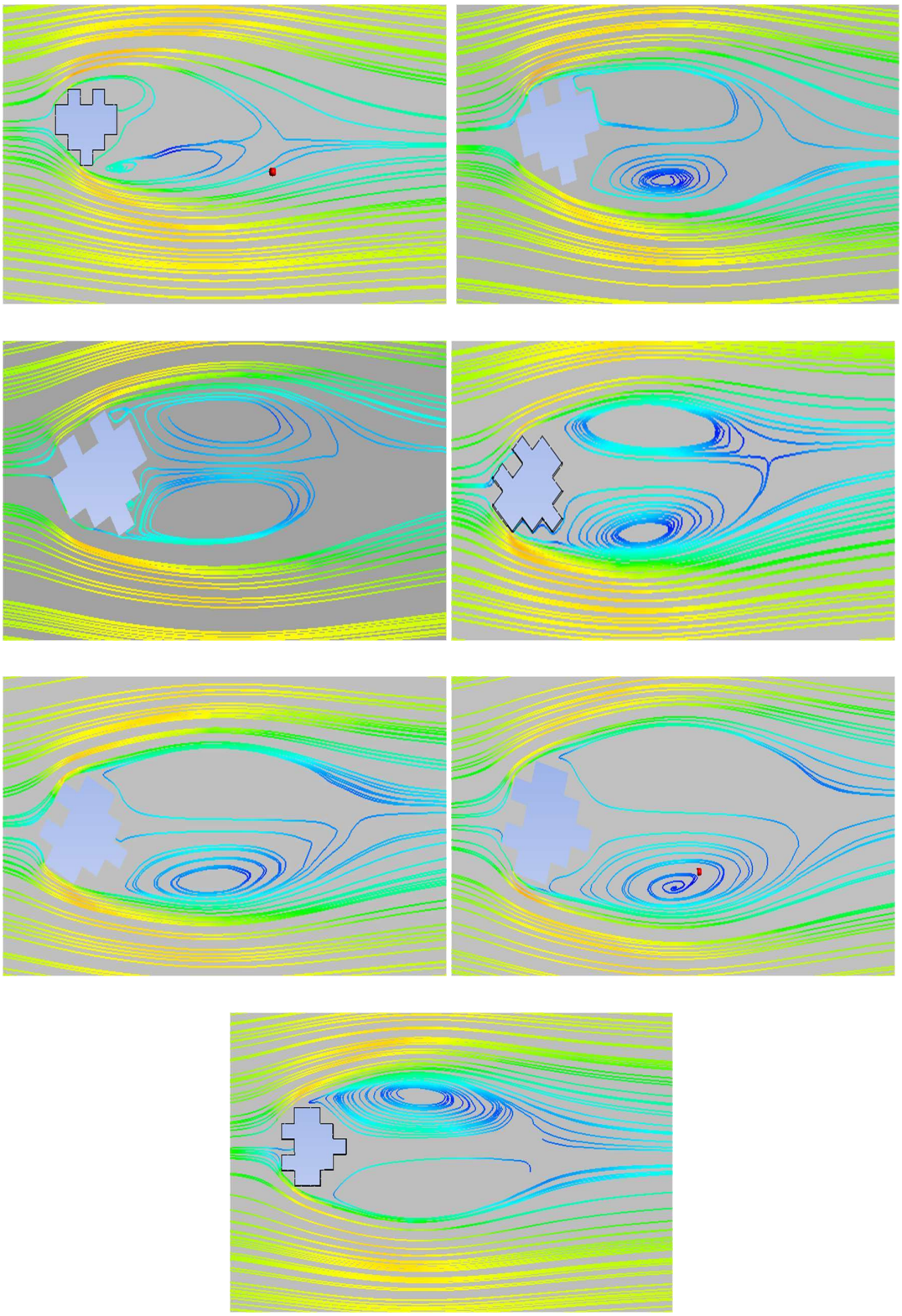

Fig 4.25. Velocity streamlines for S2 at different wind incidence angle

In case of S2, symmetrical flowlines are not observed at any angles. Greater amount of flow separation and larger vortex is formed at 60°. Higher swirling motion is obtained at an angle of 135°. The streamlines are very closely spaced at 45°, which indicates very high velocity at this angle.

The flow patterns in streamlines are given different colours to indicate the velocity at particular location and the range of each colour is provided below:

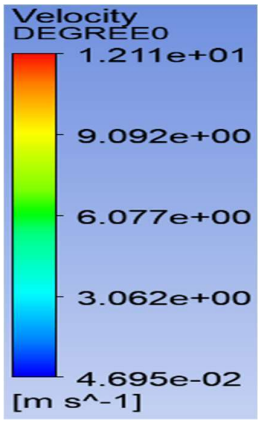

Fig 4.26. Flow velocity ranges

Taking the streamlines for S1 at 0°, the wind is approaching the structure at a higher velocity, which is reduced at the point of flow separation. As a result of which vortex is formed at this section.

4.1.4 EFFECT OF INTERFERENCE ON C_p VALUES OF S1 AND S2

Both the models 1 and 2 are simulated for the interference conditions. The Cp value for every face at every wind incidence angle is taken for all the four interference conditions. A graph is plotted to compare the variation of Cp for the structure under interference effect and isolated building. 0°, 45°, 90°, 135° and 180° angles are considered and is shown below:

4.1.4.1 INTERFERENCE EFFECT ON S1

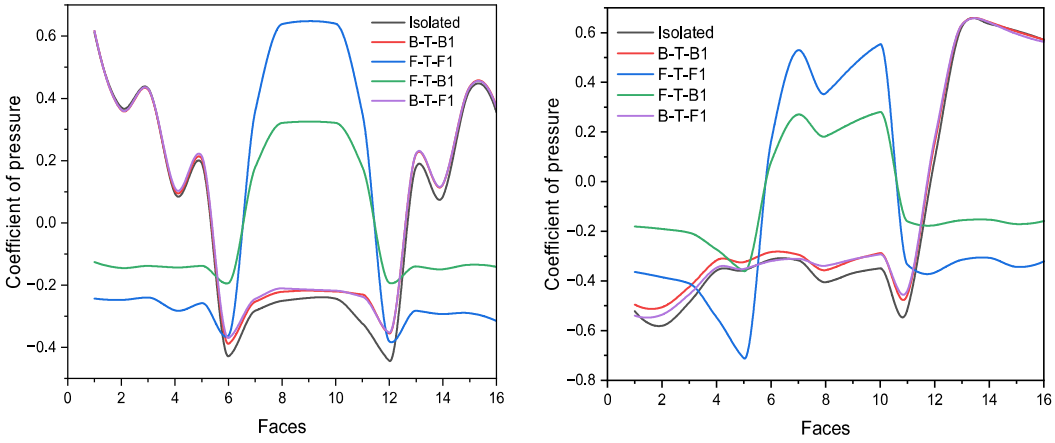

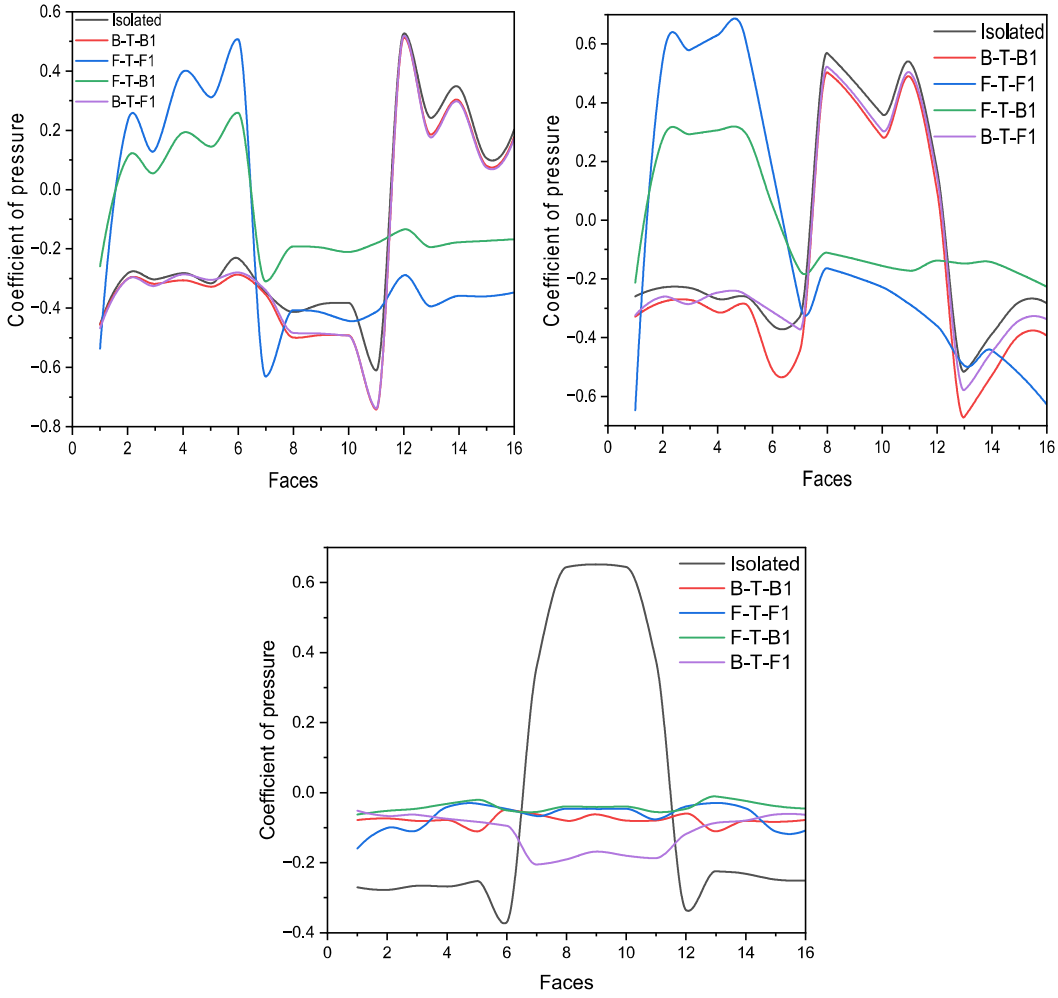

Fig 4.27. Comparison of C_p at all cases for S1

4.1.4.1.1 Front-to-Front:

- In case of F-F interference condition, the maximum value of C_p 0.66 is observed in case of **face B** at 165° and minimum value -0.82 in case of **face A** at 105°.
- Taking the C_p value of faces at 0°, the maximum value is observed on **face I** (0.65) and the minimum value is observed on **face L** (-0.38).
- At 180°, the maximum value is observed on **face M** (-0.03) and minimum value on **face A** (-0.16).

4.1.4.1.2 Back-to-Back

- In case of B-B interference condition, the maximum value of C_p 0.65 is observed in case of **face O** at 30° and minimum value -0.74 in case of **face K** at 90°.

- Taking the C_p value of faces at 0°, the largest value is observed on **face A** (0.62) and the smallest value is observed on **face F** (-0.39).
- At 180°, the largest value is observed on **face F** (-0.05) and smallest value on **face E** (-0.11).

4.1.4.1.3 Front-to-Back

- In case of F-B interference condition, the maximum value of C_p 0.33 is observed in case of **face I** at 15° and minimum value -0.37 in case of **face A** at 105°.
- Taking the C_p value of faces at 0°, the maximum value is observed on **face I** (0.32) and the minimum value is observed on **face F** (-0.19).
- At 180°, the maximum value is observed on **face M** (-0.01) and minimum value on **face A** (-0.06).

4.1.4.1.4 Back-to-Front

- In case of B-F interference condition, the maximum value of C_p 0.65 is observed in case of **face O** at 30° and minimum value -0.74 in case of **face A** at 60°.
- Taking the C_p value of faces at 0°, the maximum value is observed on **face A** (0.62) and the lowest value is observed on **face F** (-0.37).
- At 180°, the maximum value is observed on **face A** (-0.05) and lowest value on **face G** (-0.21).

Table summarizing the C_p values for S1 is given below:

Table 4.1. C_p value for S1 at 0°

Conditions	C_p	
	Max	Min
Isolated	0.61	-0.43
F-F	0.65	-0.38
B-B	0.62	-0.39
F-B	0.32	-0.19
B-F	0.62	-0.37

Table 4.2. C_p value for S1 at 180°

Conditions	C_p	
	Max	Min
Isolated	0.65	-0.37
F-F	-0.03	-0.16
B-B	-0.05	-0.11
F-B	-0.01	-0.06
B-F	-0.05	-0.21

4.1.4.2 INTERFERENCE EFFECT ON S2

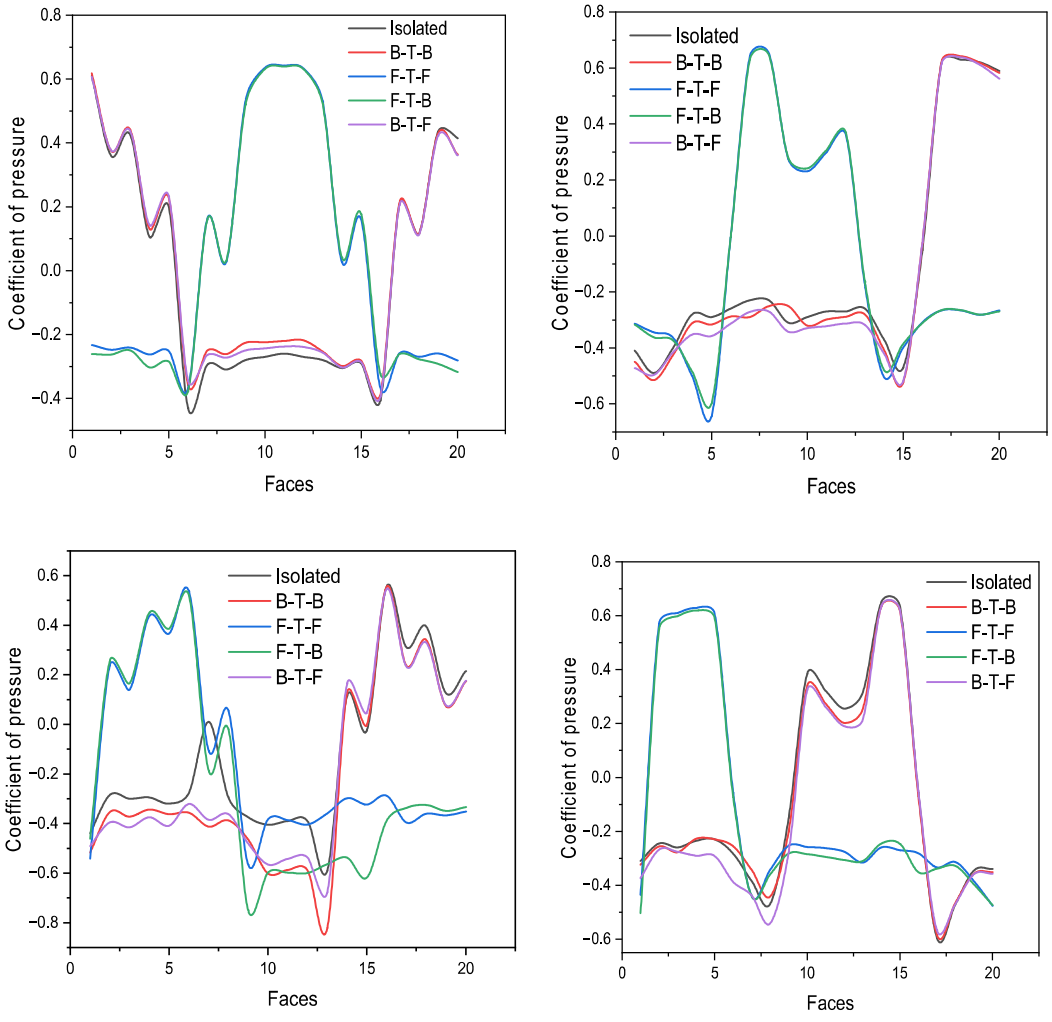

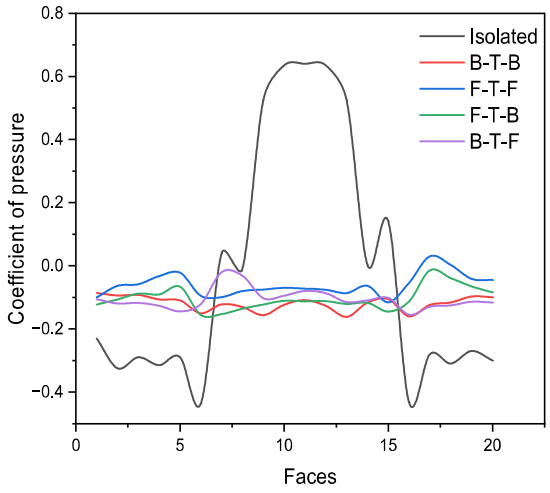

Fig 4.28. Comparison of C_p at all cases for S2

4.1.4.2.1 Front-to-Front:

- In case of F-F interference condition, the maximum value of C_p 0.65 is observed in case of **face B** at 165° and minimum value -0.49 in case of **face A** at 105°.
- Taking the C_p value of faces at 0°, the maximum value is observed on **face K** (0.64) and the minimum value is observed on **face F** (-0.37).
- At 180°, the maximum value is observed on **face Q** (0.03) and minimum value on **face O** (-0.12).

4.1.4.2.2 Back-to-Back

- In case of B-B interference condition, the maximum value of C_p 0.64 is observed in case of **face S** at 30° and minimum value -0.84 in case of **face M** at 90°.
- Taking the C_p value of faces at 0°, the largest value is observed on **face A** (0.62) and the smallest value is observed on **face P** (-0.39).
- At 180°, the largest value is observed on **face A** (-0.09) and smallest value on **face M** (-0.16).

4.1.4.2.3 Front-to-Back

- In case of F-B interference condition, the maximum value of C_p 0.65 is observed in case of **face M** at 15° and minimum value -0.39 in case of **face A** at 105°.
- Taking the C_p value of faces at 0°, the maximum value is observed on **face K** (0.64) and the minimum value is observed on **face F** (-0.38).

- At 180°, the maximum value is observed on **face Q** (-0.01) and minimum value on **face F** (-0.16).

4.1.4.2.4 Back-to-Front

- In case of B-F interference condition, the maximum value of C_p 0.62 is observed in case of **face S** at 30° and minimum value -0.44 in case of **face A** at 60°.
- Taking the C_p value of faces at 0°, the maximum value is observed on **face A** (0.61) and the lowest value is observed on **face P** (-0.39).
- At 180°, the maximum value is observed on **face G** (-0.02) and lowest value on **face P** (-0.16).

Table summarizing the C_p values for S2 is given below:

Table 4.3. C_p value for S2 at 0°

Conditions	C_p	
	Max	Min
Isolated	0.61	-0.43
F-F	0.64	-0.37
B-B	0.62	-0.39
F-B	0.64	-0.38
B-F	0.61	-0.39

Table 4.4. C_p value for S2 at 180°

Conditions	C_p	
	Max	Min
Isolated	0.64	-0.44
F-F	0.03	-0.12
B-B	-0.09	-0.16
F-B	-0.01	-0.16
B-F	-0.02	-0.16

4.1.5 DRAG FORCE COEFFICIENTS FOR S1 AND S2

The drag force coefficient is the resistance experienced by a structure due to the flow of wind. The force acting on all the faces is taken and is summed up to determine the drag force coefficient. The drag force coefficient for various wind incidence angle is calculated and is shown in table below:

Table 4.5. C_d value for S1 at different angles

Angle of incidence (°)	C_d
0°	0.69
15°	0.65
30°	0.47
45°	0.74
60°	0.91
75°	1.13
90°	1.34
105°	0.67
120°	0.49
135°	0.75
150°	0.86
165°	0.83
180°	1.04

The graph plotting C_d for S1 and S2 are given below:

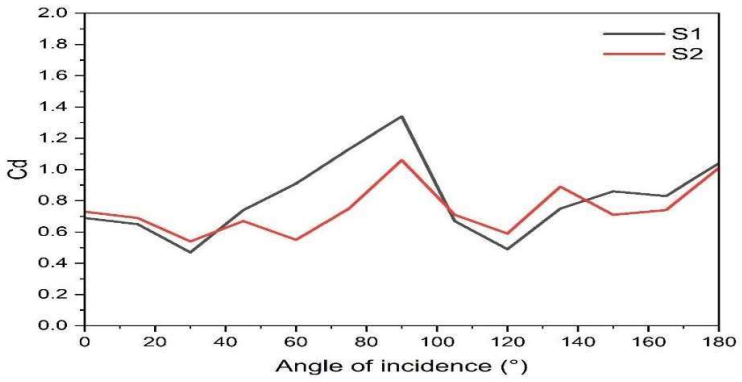

Fig 4.29. Variation of C_d for S1 and S2

Table 4.6. C_d value for S2 at different angles

Angle of incidence (°)	C_d
0°	0.73
15°	0.69
30°	0.54
45°	0.67
60°	0.55
75°	0.75
90°	1.06
105°	0.71
120°	0.59
135°	0.89
150°	0.71
165°	0.74
180°	1.01

In case of S1, the maximum value of C_d (1.34) is obtained for an angle of 90° and the minimum value (0.47) is obtained in case of 30°. The case is similar with S2, where the maximum value (1.06) is obtained for an angle of 90° and minimum value (0.54) is obtained for an angle of 30°.

CHAPTER 5

CONCLUSIONS

The simulation results have been presented through graphs, tables, contours and streamlines. The data has been interpreted and the following conclusions are obtained:

- The validation of the square model gives satisfactory results with respect to 1S:875 (Part III)- 2015.
- Two different structures having almost same geometry, height and area shows variation in overall pressure distribution due to difference in corner cuts. But, the variation of C_p with wind incidence angle is similar for some of the common faces.
- The velocity streamlines and pressure contours changes with wind incidence angles. From the pressure contours, the increase in pressure with height is clearly visible. The suction zone and vortex formation in both the models are interpreted using the streamlines.
- In isolated condition, it can be clearly observed that the maximum positive pressure coefficient is observed on the wind ward side when the building face is in perpendicular to wind direction.
- Buildings under interference effect shows better performance than an isolated building under same wind conditions.
- At 0° and 180°, F-F interference condition gives the higher positive coefficient of pressure and the lowest suction.
- Comparing the buildings for isolated condition and under interference effect, Front to Front condition is found to be more effective under same wind conditions.
- Highest drag force coefficient (1.34) is obtained in case of S1 at 90° and lowest (0.47) is also obtained in case of S1 at 30°.

- Numerical simulation aids as an effective tool to determine the performance of an irregular shaped high- rise buildings, as there are no standard codal provisions to find the same.

FUTURE SCOPE OF THE WORK

Most of the parameters in this study is done for isolated conditions. The streamline patterns can be determined also for interference effect, as the presence of an adjacent building will cause a high difference in flow patterns. Also, the drag coefficient and lift coefficients can be determined for interference cases. The parameters used in this study can be used for the analysis of similar shapes in future.

REFERENCES

[1] "IS-875-part-3-2015".

[2] R. Sheng, L. Perret, I. Calmet, F. Demouge, and J. Guilhot, "Wind tunnel study of wind effects on a high-rise building at a scale of 1:300," *Journal of Wind Engineering and Industrial Aerodynamics*, vol. 174, pp. 391–403, Mar. 2018, doi: 10.1016/j.jweia.2018.01.017.

[3] S. Bhattacharjee, S. Banerjee, S. G. Majumdar, A. Dey, and P. Sanyal, "Effects of Irregularity on a Butterfly Plan-Shaped Tall Building under Wind Load," *Journal of The Institution of Engineers (India): Series A*, vol. 102, no. 2, pp. 451–467, Jun. 2021, doi: 10.1007/s40030-021-00511-6.

[4] G. T. Bitsuamlak, "Shape effects on the wind-induced response of high-rise buildings Numerical and experimental simulation of tornado-like vortices View project Probabilistic Performance-Based Wind Design of Tall Mass-Timber Buildings View project." [Online]. Available: https://www.researchgate.net/publication/271198030

[5] Y. Li, Q. S. Li, and F. Chen, "Wind tunnel study of wind-induced torques on L-shaped tall buildings," *Journal of Wind Engineering and Industrial Aerodynamics*, vol. 167, pp. 41–50, Aug. 2017, doi: 10.1016/j.jweia.2017.04.013.

[6] M. Gu, "Wind-resistant studies on tall buildings and structures," *Sci China Technol Sci*, vol. 53, no. 10, pp. 2630–2646, 2010, doi: 10.1007/s11431-010-4016-2.

[7] B. Bhattacharyya and A. Kumar Ahuja, "Wind Induced Pressure on 'E' Plan Shaped Tall Buildings Aerodynamic shape modification of 'Y' plan shaped tall building View project Concrete filled Tube View project," 2014. [Online]. Available: https://www.researchgate.net/publication/264548132

[8] J. Yi and Q. S. Li, "Wind tunnel and full-scale study of wind effects on a super-tall building," *J Fluids Struct*, vol. 58, pp. 236–253, Oct. 2015, doi: 10.1016/j.jfluidstructs.2015.08.005.

[9] S. Chakraborty, S. K. Dalui, and A. K. Ahuja, "Wind load on irregular plan shaped tall building - A case study," *Wind and Structures, An International Journal*, vol. 19, no. 1, pp. 59–73, 2014, doi: 10.12989/was.2014.19.1.059.

[10] R. Paul and S. K. Dalui, "Wind effects on 'Z' plan-shaped tall building: a case study," *International Journal of Advanced Structural Engineering*, vol. 8, no. 3, pp. 319–335, Sep. 2016, doi: 10.1007/s40091-016-0134-9.

[11] R. Raj and A. Kumar Ahuja, "Wind Loads on Cross Shape Tall Buildings," *Journal of Academia and Industrial Research*, vol. 2, no. 2, 2013.

[12] R. Jb and J. Zurafiski, "Wind tunnel investigations of interference effects on pressure distribution on a building," 1995.

[13] P. J. Oliveira and B. A. Younis, "On the prediction of turbulent #ows around full-scale buildings," 2000.

[14] R. G. Patel and S. D. Ramani, “PARAMETRIC STUDY TO UNDERSTAND PRESSURE DISTRIBUTION AROUND DIFFERENTIAL HEIGHT STRUCTURE.” [Online]. Available: www.ijariie.com

[15] S. Mukherjee, S. Chakraborty, S. K. Daluf, and A. K. Ahuja, “Wind induced pressure on ‘Y’ plan shape tall building,” *Wind and Structures, An International Journal*, vol. 19, no. 5, pp. 523–540, Nov. 2014, doi: 10.12989/was.2014.19.5.523.

[16] S. K. Verma, A. K. Ahuja, and A. D. Pandey, “Effects of wind incidence angle on wind pressure distribution on square plan tall buildings,” *J. Acad. Indus. Res*, vol. 1, no. 12, p. 747, 2013.

[17] E. Kumar Bandi *et al.*, “Number 3 Paper Type: 1. Book chapter/Part chapter 2,” 2013. [Online]. Available: www.ctbuh-korea.org/ijhrb/index.php

[18] R. R. Ahirwar, “Article in Wind and Structures An International Journal ·,” *Wind and Structures*, vol. 31, no. 5, pp. 441–453, 2021, doi: 10.12989/was.2020.31.5.441.

[19] R. Kar and S. K. Dalui, “Wind interference effect on an octagonal plan shaped tall building due to square plan shaped tall buildings,” *International Journal of Advanced Structural Engineering*, vol. 8, no. 1, pp. 73–86, Mar. 2016, doi: 10.1007/s40091-016-0115-z.

[20] S. Pal, R. Kumar Meena, R. Raj, and S. Anbukumar, “Wind tunnel study of a fish-plan shape model under different isolated wind incidences,” *Wind and Structures, An International Journal*, vol. 33, no. 5, pp. 353–366, Nov. 2021, doi: 10.12989/was.2021.33.5.353.

[21] R. K. Meena, R. Raj, and S. Anbukumar, “Wind Excited Action around Tall Building Having Different Corner Configurations,” *Advances in Civil Engineering*, vol. 2022, 2022, doi: 10.1155/2022/1529416.

[22] A. Kumar and R. Raj, “Study of pressure distribution on an irregular octagonal plan oval-shape building using cfd,” *Civil Engineering Journal (Iran)*, vol. 7, no. 10, pp. 1787–1805, Oct. 2021, doi: 10.28991/cej-2021-03091760.

[23] P. K. Goyal, S. Kumari, S. Singh, R. K. Saroj, R. K. Meena, and R. Raj, “Numerical Study of Wind Loads on Y Plan-Shaped Tall Building Using CFD,” *Civil Engineering Journal (Iran)*, vol. 8, no. 2, pp. 263–277, Feb. 2022, doi: 10.28991/CEJ-2022-08-02-06.

[24] K. Ming Lam, K. Lam, and J. Zhao, “Interference effects on wind loads on a row of tall buildings Investigation of heavy particles behavior in turbulence View project Building wakes View project Interference effects of wind loads on a row of tall buildings,” 2006. [Online]. Available: https://www.researchgate.net/publication/242071345

[25] L. Sobankumar, S. Prabavathy, and R. Vigneshwaran, “Study on wind flow around a pentagon plan shape tall building using CFD,” in *Journal of Physics: Conference Series*, IOP Publishing Ltd, Jul. 2021. doi: 10.1088/1742-6596/1850/1/012045.

[26] A. K. Bairagi and S. K. Dalui, “Estimation of Wind Load on Stepped Tall Building Using CFD Simulation,” *Iranian Journal of Science and Technology - Transactions of Civil Engineering*, vol. 45, no. 2, pp. 707–727, Jun. 2021, doi: 10.1007/s40996-020-00535-1.

[27] R. Raj, A. Sharma, and S. Chauhan, “Response of Square and Plus Shaped Buildings on Varying Wind Loads,” in *Urbanization Challenges in Emerging Economies: Resilience and Sustainability of Infrastructure - Selected Papers from the ASCE India Conference 2017*, American Society of Civil Engineers (ASCE), 2018, pp. 206–215. doi: 10.1061/9780784482032.022.

[28] R. K. Meena, R. Raj, and S. Anbukumar, “Comparative Study of Wind Loads on Tall Buildings of Different Shapes,” in *Lecture Notes in Mechanical Engineering*, Springer Science and Business Media Deutschland GmbH, 2023, pp. 225–235. doi: 10.1007/978-981-19-3410-0_18.

[29] M. S. Thordal, J. C. Bennetsen, and H. H. H. Koss, “Review for practical application of CFD for the determination of wind load on high-rise buildings,” *Journal of Wind Engineering and Industrial Aerodynamics*, vol. 186, pp. 155–168, Mar. 2019, doi: 10.1016/j.jweia.2018.12.019.

[30] J. Revuz, D. M. Hargreaves, and J. S. Owen, “On the domain size for the steady-state CFD modelling of a tall building,” *Wind and Structures, An International Journal*, vol. 15, no. 4, pp. 313–329, 2012, doi: 10.12989/was.2012.15.4.313.

LIST OF PUBLICATIONS

1. Mohanan, A.S., Sharma,D., Raj,R. (2023), “ Analysis of wind effect on tall buildings of irregular cross-sections using numerical simulation” . International Conference on Advances in Civil Engineering (ICACE,2022).

International Conference on Advances in Civil Engineering 2022

Certificate

ICACE
20-22 DEC 2022

This is to certify that the paper entitled

Analysis of Wind Effect on Tall Buildings of Irregular Cross-Section Using Numerical Simulation

authored by

Arya S M, Deepak Sharma, Ritu Raj

is presented in the International Conference on Advances in Civil Engineering 2022 held on 20-22 December 2022, organized by Technology Research and Innovation Centre, India and hosted by LSKBJ College of Engineering, Chandwad, Nashik, India

Dr. Sandip A. Kale
Technical Committee Chair

Dr. Yuvaraj L. Bhirud
Chairperson

Dr. K Jagannadha Rao
Chairperson

Dr. Mahadeo D. Kokate
Principal, LSKBJ COE Chandwad, India

LSKBJ College of Engineering, Chandwad, Nashik, India

Chaitanya Bharathi Institute of Technology (A), Hyderabad, India

Technology Research and Innovation Centre, India

Academy of Nanotechnology and Waste Water Innovations, SA

Accra Technical University, Ghana

SGM College of Engineering, Mahagaon, India